

# Journal of Climate

## Locally and remotely forced subtropical AMOC variability: A matter of time scales --Manuscript Draft--

Manuscript Number:	JCLI-D-19-0844
Full Title:	Locally and remotely forced subtropical AMOC variability: A matter of time scales
Article Type:	Article
Corresponding Author:	Quentin Jamet Florida State University Tallahassee, UNITED STATES
Corresponding Author's Institution:	Florida State University
First Author:	Quentin Jamet
Order of Authors:	Quentin Jamet William K. Dewar Nicolas Wienders Bruno Deremble Sally Close Thierry Penduff
Abstract:	<p>Mechanisms driving the North Atlantic Meridional Overturning Circulation (AMOC) variability at low-frequency are of central interest for accurate climate predictions. Although the subpolar gyre region has been identified as a preferred place for generating climate time scales signals, their southward propagation remains under consideration, complicating the interpretation of the observed time series provided by the RAPID-MOCHA-WBTS program. In this study, we aim at disentangling the respective contribution of the local atmospheric forcing from signals of remote origin for the subtropical low-frequency AMOC variability. We analyze for this a set of four ensembles of a regional (20S-55N), eddy-resolving (1/12) North Atlantic oceanic configuration, where surface forcing and open boundary conditions are alternatively permuted from fully varying (realistic) to yearly repeating signals. Their analysis reveals predominance of local, atmospherically forced signal at interannual time scales (2-10 years), while signals imposed by the boundaries are responsible for the decadal (10-30 years) part of the spectrum. Due to this marked time scale separation, we show that, although the intergyre region exhibits peculiarities, most of the subtropical AMOC variability can be understood as a linear superposition of these two signals. Finally, we find that the decadal scale, boundary forced AMOC variability has both northern and southern origin, although the former dominates over the latter, including at the site of the RAPID array (26.5N).</p>

Responses to the reviewers for the paper

## **"Locally and remotely forced subtropical AMOC variability: A matter of time scales"**

by Quentin Jamet, William K. Dewar, Nicolas Wienders, Bruno Deremble, Sally Close and Thierry Penduff

We thank the editor for handling this revision, and the reviewers for their interest in our study and for the quality of their comments. Our detailed responses follow. Reviewers comments are indicated in **bold**, and our responses are marked with a "→". In the "tracked changes" version of the revised manuscript (see the Additional Material for Reviewer Reference), we have highlighted the significant corrections from the previous version, in response to the reviewers comments, by highlighting them in bold characters.

### **Detailed responses to reviewer #1:**

The authors identified respective roles of surface vs remote forcing on the AMOC low frequency variability in the subtropical North Atlantic and found a timescale dependency: local atmospheric forcing is responsible for AMOC variability on interannual time scales whereas remote forcing from the subpolar latitudes is responsible for AMOC variability on decadal time scales. While this conclusion is not totally original, the fact that the authors used an eddy-resolving model for the sensitivity experiments and an ensemble approach is a welcome development. The manuscript is written clearly, and the conclusions are sound (for the most part) given the evidences presented. I therefore recommend its acceptance for publication after a minor revision. I only have a few specific comments below, mostly asking for clarification.

### **Specific Comments:**

**Line 81-82, "... contributed to about 0.2 Sv of the lower limb AMOC decadal variability"** Please indicate what is the expected amplitude of "lower limb AMOC decadal variability" with proper references, so the readers can know if 0.2 Sv is a big contribution or not.

→ Thank you for this comment. For reference, we have provided the estimations of the lower limb AMOC variability as measured by the RAPID-MOCHA-WBTS array, i.e.  $\sim O(1 \text{ Sv})$ .

lines 87-88: "*which may well contribute to about 10-20% of the  $\sim O(1 \text{ Sv})$  low-frequency variability measured by the RAPID array (Smeed et al. 2014,2018).*"

**L124-125, "36 minutes relaxation time scale", L128, "1 day relaxation time"** These are very short relaxation time scales, I think. Are they typical of other regional model configurations? What is your regional model's time step? Could you provide some references on boundary forcing relaxation time scale typically used?

→ Thank you for this comment. The model time step is 200 seconds, thus the relaxation times scales span several time steps. We have added a comment on the relaxation times scales of our boundary conditions:

lines 140-141 : "*Although these relaxation times scales are relatively short, no adverse effects were apparent upon inspection.*"

**Line 141, "The 12 initial conditions are common to all ensembles,"** At first, I was confused by this sentence (initial conditions must be different for a different ensemble

member) but then I realized what you meant is that the same set of I.C. is used across the different experiments. Please clarify.

→ We have clarified this misleading point, thank you.

lines 158-159: *"This set of 12 initial conditions is used across the four different ensembles, such that initial perturbations are the same in all experiments."*

Line 158-159, "climatological open boundary conditions..." Please specify the time scales of climatology, as climatology can be defined on many time scales, from sub-daily to daily, monthly or even longer. It's possible that I missed it, but I could not find anywhere in the paper what is the time scale of your 'climatology'.

→ We have clarified our procedure to derive climatological boundary conditions by stating:

lines 176-177: *"i.e. 5-day open boundary conditions are averaged across the years to provide a mean representation of the seasonal cycle."*

Lines 387-400, the whole paragraph I don't get what you are trying to convey here... What "basin mode" do you mean? Why can it not be excluded? Is it some numerical artefact or a physical mode? Please clarify.

→ Thank you for this comment. We referred here to modes that would develop to adjust to changes in the boundary conditions when permuting open boundary or surface forcing from realistic to yearly repeating signals. We have clarified this point in the text:

lines 412-415: *"Permuting open boundaries and surface forcing from realistic to yearly repeating signals induces an imbalance between the state of the ocean and the applied new boundary conditions. To adjust, the ocean is likely to generate wave-like signals in response to these changes, such that we cannot exclude the presence of artificial modes in our regional configuration."*

Line 480-483, "... suggesting a weak contribution..... and pace AMOC variability further north". How could a weak contribution pace the variability further north? 0.1-0.2 Sv is weak relative to the 1-2 Sv anomalies associated with decadal variability of the AMOC in the North Atlantic.

→ Thank you for this comment. Our point here is that, even if their imprint is weak, South Atlantic low-frequency signals are able to contribute to the AMOC variability in the North Atlantic sector, thus crossing the equator. To our knowledge, the mechanisms behind this northward propagation remain unclear and would deserve further investigations. To avoid confusion, we have replaced "pace" by "contribute".

Lines 544-550, These ending remarks are not convincing. Fig. 4 lower-right panel and Fig. 5 lower- right panel both show discrepancies between the reconstructed and full time series, so you can't really say "we found that the linear reconstruction leads to consistent estimates of the realistic low-frequency AMOC variability".

→ Thank you for this comment. Note that the beginning of this sentence points to the subtropical gyre only, while the mentioned discrepancies are found at the intergyre, which we discuss at the beginning of this paragraph. Also note that these discrepancies appear in given frequency bands, such that the correlations between the time series remain high. The new Fig. 7 shows a map of these correlations, where correlations of  $r = 0.9$  and larger are found in most of the subtropical gyre.

#### Editorial:

Line 181, "than" is a typo? It should be "that"

Line 243, "PCA" This is the first time you used PCA, please spell it out

Line 253, now you can use PCA (instead of spelling it out)

Line 280, "of a local", change "of" to "to"

Line 471, add "North" before "Atlantic", there are subpolar latitudes in the SH

→ Thank you for these editorial suggestions.

## Detailed responses to reviewer #2:

### Specific Comments:

The authors analyze four ensembles of a 1/12 regional ocean model (MIT gcm) to investigate the role of local forcing (surface) and remote forcing (open ocean boundaries) in driving interannual to decadal anomalies in the intensity of the Atlantic Meridional Overturning Circulation (AMOC) at subtropical latitudes. A focus is made at 26.5N, where long-term observational record of the AMOC are available. Each ensemble reflects specific forcing conditions with the surface and/or boundary forcing being either "realistic" or "climatologic". The paper main message is the predominance of local (resp. remote) forcing on interannual (resp. decadal) time scales, enabling a simple linear superposition of these two components in the subtropical band. The primary role of the northern North Atlantic in feeding the subtropical decadal signal is also pointed out, and discussion about the intrinsic (vs. forced) part of the variability provided.

It was a pleasure to read this manuscript. It is concisely and well written, with the aim and underlying motivations clearly stated in the introduction and easy to grasp from the first read. The whole analysis (methods, results and conclusion) is presented in a comprehensive way, with adequate figures and clear description/interpretation. The methodology is (to my knowledge) new and original, although the authors could make even clearer the added value of their results to the literature. I believe this piece of work could be an important (modelling) reference for understanding observation-based monitoring of the AMOC, at 26.5N, and more generally to support current efforts that are made to understand its meridional coherence across the whole North Atlantic. My comments are consequently mostly minor but yet important for making the manuscript clearer to non-specialist readers. I recommend this paper for publication in Journal of Climate.

### Minor Comments:

**1. 56:** The authors could precise what they mean by "decadal scale dynamics".

→ Thank you for this comment, we have further detailed this dynamics:

lines 60-61: " *such as deep water formation rates or the longer time it takes for baroclinic Rossby waves to cross the basin at higher latitudes (Wunch and Heimbach, 2013).*

**1.73:** I am not too sure that the weak subpolar-subtropical connectivity of the deep AMOC limb is something shown in Lozier et al 2019.

→ Thank you for this referential comment. Fig. 3 of Lozier et al 2019 exhibits a weak AMOC variability at OSNAP West, suggesting a weak connectivity between deep water formation within the Labrador Sea and the AMOC. They also discuss this point in the text and in the conclusion. We thus prefer to keep this reference as it is.

**1. 92-95:** I am a little puzzled because this statement sounds pretty much like the main result of the present study, with buoyancy forcing in the Labrador Sea (or SPG as a whole) in the study of Biastoch et al (2008) being replaced by open ocean boundary forcing at 55N here. I think the authors must be clearer on what dissociate these two studies.

→ Thank you for this valuable comment. Our study differs from earlier studies by the use of eddy-resolving ensemble simulations. We have clarified this point in the introduction:

lines 104-107: " *But these studies have also pointed out the potential sensitivity of this linear superposition to the presence of oceanic eddies. We thus propose here to further analyze this linear superposition in such an eddying regime.* ".

We have also discussed the benefits of the ensemble strategy in Section 4c, supported by the new

Fig. 7, in comparison with single simulation sensitivity experiments.

**1. 122: Are the results of the paper sensitive to the choice of the domain northern boundary (55N)?**

→ The northern boundary at 55°N has been selected for two reasons. First, it remains south of areas where sea-ice cover is likely to form, thus removing the need for a sea-ice model. Second, it remains far enough from the separated Gulf Stream to allow its unconstrained evolution. Additionally, the fraction of variability that is intrinsic in the latitudinal range from 48°N to 62°N is small (Grégorio et al 2015), such that the underestimated intrinsic variability induced by the prescription of open boundary conditions at this latitude is expected to be weak. Although we have not conducted sensitivity experiments to the northern boundary, we do not anticipate major sensitivities of the subtropical AMOC variability to the location of that boundary.

**1. 158: the term "low-frequency" can be a bit vague. Maybe the actual temporal scales could be mentioned.**

→ Thank you, we have replaced "low-frequency" by "interannual-to-decadal". Also note that we provide details on the time scale of interest in this study at the end of the section (line 214), i.e. from 2 years to 30 years.

**1. 182: explanation**

→ Thank you. Done.

**1. 206: the authors refer to observations to validate their AMOC structure without providing the references.**

→ Thank you. Such comparisons have been published by Jamet et al (2019) for the ensemble ORAR. We have added the appropriate reference.

Lines 226-227: *"Further comparisons of the ensemble mean AMOC and the RAPID-MOCHA-WBTS observational estimates can be found in the Supporting Information of Jamet et al (2019b)."*

**1. 263: that**

→ Thank you. Done.

**1. 275-276: what would be the reason for the OCAC ensemble to be more energetic at decadal time scales (and reach a kind of plateau from about 10 years)?**

→ Thank you for this interesting comment. We suspect the presence of a more energetic AMOC variability at decadal time scale in this ensemble to reflect the too short decorrelation time scales of our initial conditions. They have been constructed through a 1-year long integration, such that any initial perturbations that may take longer than 1 year to develop are not considered. This interpretation is further supported by the horizontal structure of the leading mode of variability (Fig. 2, bottom right panel), which strongly resembles the leading mode of intrinsic AMOC variability identified in our ensembles (Fig. 6). To investigate this question, we have run additional ensemble members for this ensemble with macro initial conditions which are meant to account for longer decorrelation time scales. Their analysis is underway and will be reported in a dedicated study.

**1. 280-281: Maybe a distinction of time scales should be made here? Again, "low-frequency" sounds a bit vague. And the statement that AMOC variability "contains little information about boundary forced signal" does not hold for decadal time scales where this boundary signals actually dominate? I suggest rephrasing here.**

→ Thank you for this comment. We recall that we are analyzing the leading mode of variability extracted through a PCA in this section, not the full AMOC time series. We agree that the full, realistic AMOC time series do contain information about boundaries at decadal time scale, but such information is not part of the leading mode of variability extracted through a PCA.

**1. 295-297: I am slightly confused as I would have said the opposite (largest difference between ORAC and OCAC than between ORAR and OCAR). Maybe rephrasing is**

needed.

→ We are not sure to clearly understand this comment. In the previous section, we have shown that the leading mode of AMOC variability in the ensemble mean ORAR mostly reflects the atmospheric forcing (it compares well with the leading mode in the ensemble OCAR, but does not compare to the leading mode in the ensemble ORAC). We drawn a similar conclusion here by analyzing full time series, where OCAR correlates well (0.8) to ORAR, but ORAC does not (0.3; see lines 377-378).

**1. 300-302: It could be worth adding the actual observation-based RAPID AMOC time series here - for further model validation and to provide the reader with some hints that the model-based mechanisms described by the authors actually "apply" in the real ocean.**

→ This is a fair statement. We have added the RAPID time series on Fig. 5 top left panel as suggested. Note however that this observational time series contains a signal due to intrinsic variability, which has been estimated to account for about 0.9 Sv (Jamet et al 2019b). A direct comparison with our ensemble means is thus not possible. We have pointed this out in the footnote on page 16.

**1. 313-315: given the fairly large % of explained variance of the first EOF modes, this is not so much surprising? In fact, the added value of Figure 4 (top) from Figure 3 is not so obvious to me. Maybe its use could be further detailed.**

→ Thank you for this comment. EOFs indeed explain a significant amount of the total variance. They do however not account for the full signal of the AMOC variability but only about half of it. To account for the full AMOC spectrum, and perform a linear reconstruction, we thus prefer to use the full time series that contain all information. It is indeed likely that a linear reconstruction based only on the EOF1s would lead to lower correlations between the reconstructed and the realistic AMOC time series. To make the separation between PCA and full time series clear, we state at the end of Section 3:

*" The PCA discussed here provides a statistical description of the main spatio-temporal patterns of AMOC variability. It however only accounts for a given fraction (about 40-50% in our ensembles) of the total signal. We thus extend our spectral analysis in the following by considering full time series to further investigate time scale separation between local atmospherically forced and remotely forced AMOC variability, and assess their linear combination for interpreting realistic time series. "*

and at the beginning of Section 4a:

*" We now wish to extend our results to full time series in order to account for the complete low-frequency AMOC spectrum."*

**1. 339-341: As mentioned in my previous comment, the added value of the present work from that of Biastoch et al (2008) should be stated more clearly.**

→ Thank you again for this valuable comment. We have further discussed the added value of our study. We have illustrated the benefits of our eddy-resolving simulations with an ensemble approach in the new section 4c and the new Fig. 7. This, we believe, brings a significant value of our study by providing a nice illustration of the benefits of ensembles strategies when dealing with eddy-resolving simulations. We thus thank again the reviewer for her/his very insightful comment.

**1. 371-375; I don't understand why this Figure 5 is described again here as it was already done some paragraphs ago.**

→ We describe the spectral estimates of the three ensemble means in Section 4a with Fig. 5, and come back to this figure in Section 4b to discuss spectral differences between the realistic and the reconstructed AMOC time series.

**1. 417-418: Maybe this is a tricky question, but why would the intrinsic mode peak at 2000m?**

→ Thank you for this very interesting question. We are unfortunately not able to provide answers yet. We are planing on further analyzing the 3-dimensional structure of the ocean circulation associated with this intrinsic mode of variability to better understand the underlying dynamics. Results will be

reported in a dedicated study.

**l. 455-457:** Those statements can be a little confusing. I may misunderstand something here, but I am not sure why the member with highest intrinsic variability is chosen, whereas the northern vs. southern comparison relates to forced variability at the boundary. I would suggest to rephrase these statements, and maybe the whole paragraph to make the methodology clearer.

→ runN and runS are single simulations, not ensemble simulations. They include both internally generated and externally forced signals. The ensemble OCAC is driven by yearly repeating surface and boundary forcing, thus no variability is expected to be driven by the forcing at time scales longer than one year. We thus use the ensemble members of this ensemble as an estimate of the variability that is intrinsically driven. We use the ensemble member with the largest variance as a representation of the largest estimate of intrinsic variability.

**l. 471: the role of the subpolar North Atlantic**

→ Thank you. Done.

**l. 503-504:** It could be worth noting (here or somewhere else) that although the AMOC decadal variability is controlled by open ocean boundary forcing in this regional model configuration, the latter is in reality also largely driven by the atmosphere (surface-forced water mass transformation in the subpolar gyre -see recent observation-based publications on the subject).

→ Thank you for this comment. The local nature of the atmospheric forcing at interannual time scale discussed in this study is made explicit in the introduction, and we have systematically referred to its local character throughout the paper.

**l. 519: within**

→ Thank you. Done.

**l. 524-527:** I am confused. Does this just contradict conclusion #4 (and line 464-465)? There are no clear hints in Figure 7 that southern-origin signals impact decadal AMOC changes in the northern subtropical gyre.

→ Thank you for this comment. We have rephrased this to avoid confusion:

lines 580-585: *"Although the sensitivity experiments on the southern or northern origin of the boundary forced AMOC variability suggest a stronger imprint of the northern boundary signal for AMOC variability at 26.5°N, they also support the earlier findings of Biastoch et al (2008) and Leroux et al (2018) where the southern boundary is found to imprint a weak AMOC variability at 26.5°N, with a likely intrinsic origin (Leroux et al, 2018)."*

**Fig 1. The bottom-right panel is not described in the text.**

→ Thank you, we have commented on this.

line 140: *"The OCAC ensemble time mean AMOC changes illustrate the combination of these two effects (bottom right panel)."*

**Fig 2. Focusing on the region north of 26.5N, the pattern of AMOC EOF1s confirm some previous hypothesis about the degree of latitudinal coherence in AMOC changes. A clear "gyre-specific" response is found for the locally-forced component, with opposed changes at subtropical and subpolar latitudes, while a meridionally-coherent mode is found for the remotely-forced component. It could be worth mentioning this and making references to previous literature of the subject.**

→ Thank you for this comment. This point was part of our original discussion on leading modes of AMOC variability. We have made it even more transparent by stating:

line 254: *"revealing the imprint of remotely-forced signals on the subtropical AMOC variability."*

line 262: *"i.e. a 'gyre-specific' mode with a sign reversal at the intergyre."*

### Detailed responses to reviewer #3:

This is an interesting paper where the authors present results from a carefully designed set of regional (Atlantic) high-resolution ensemble simulations. The experimental setup allows the authors to estimate whether the origin of AMOC variability is due to atmospheric forcing or to variability at the southern and northern boundaries (20S / 55N). The main conclusion is that on timescales shorter than 10 years the local atmospheric forcing is the main driver. However, on decadal timescales the main contribution to AMOC variability is linked to the conditions imposed at the northern and southern boundaries of the Atlantic domain. The results also show that a linear combination of the AMOC variability due to local atmospheric forcing and of the variability originating from the southern and northern boundary can explain most of the total AMOC variability.

I think this study provides valuable new insight into the origin of decadal AMOC variability and is a nice attempt to disentangle local from remote variability sources for the AMOC in the North Atlantic. The paper is largely clear and well-written. However, there are aspects that I feel require some attention (see comments below). I also noted that there are numerous typos and grammatical errors and I'd encourage the authors to carefully proof read their manuscript as part of their revision.

In summary, I think that this study will be a good contribution to Journal of Climate once the points listed below have been addressed and I recommend publication subject to minor revisions.

#### Main point:

I feel that the role played by the southern boundary in the ensemble experiments should be discussed more carefully. The interpretation of the experiments ORAR, OCAR, ORAC and OCAC is that local (atmospheric) forcing dominates timescales of 2-10 years whereas the southern/northern boundaries dominate timescales from 10-30 years.

→ Thank you for this comment. We would like to first recall here that our study focuses on the AMOC variability within the North Atlantic subtropical gyre, for which we draw out our conclusions. We have worked on discussing the effect of the southern boundary more carefully throughout the paper. Responses to specific comments follow below.

Following the authors' explanations  $\langle \text{ORAC} \rangle$  should contain hardly any high frequency variability. However, when I look at Fig. 7 I'd say that this is only true North of the Equator. In the South Atlantic I can see that the ensemble average  $\langle \text{ORAC} \rangle$  still contains quite a large variability south of the Equator on interannual timescales (coherent meridional bands between 20S and the Equator Fig. 7 top left). By eye at least this variability seems as large as the lower frequency variability seen in the northern hemisphere. Why is this variability hardly seen in the PSD function shown for ORAC in Figure 5? Has this variability been filtered out (by eye it would seem that some of it is on timescales shorter than 2 years). I note here that in Figure 2 the leading EOF suggests a large variability in the South Atlantic (the only of the 4 cases where variability seems to be of similar magnitude in both North and South Atlantic)

→ The time scale separation between local, atmospherically and boundary forced signals discussed in this paper holds for the North Atlantic subtropical AMOC variability, our region of interest. Nonetheless, we agree that south of the equator, the southern boundary imprints a signal at interannual time scales, as revealed by EOF1 (Fig. 2) and the Hovmöller diagram (Fig. 9) of the ensemble mean ORAC. Spectral estimates reveal a relatively sharp peak around 2 years, which is smoothed by the 5-point moving averaging. However, after inspection of the non-filtered PSD, we found that this South Atlantic signal remains weaker than the decadal time scale variability of the subtropical North

Atlantic AMOC variability. We have commented on this in Section 6 when describing the imprint of the southern boundary south of the equator:

lines 532-535: " *In contrast with the northern boundary, the signal imprinted by the southern boundary contains energy at interannual time scales. This is visible in the Hovmöller diagrams of both the ensemble mean  $\langle \text{ORAC} \rangle$  and of runS, as well as in the spectral estimates of AMOC variability of Fig.5, bottom left panel.* "

The interannual variability seen for ORAC in Figure 7 cannot have an atmospheric origin and must result from the boundary conditions imposed at the southern boundary. There is a hint of higher frequency variability in the Northern Hemisphere as well but as the authors say this variability is small and likely a reflection that the ensemble mean over 12 members is probably not sufficient to average out the intrinsic variability originating between about 35-40N. The amplitude of the interannual variability is much larger in the South Atlantic. My feeling is that this southern variability reflects intrinsic variability present in the conditions imposed at the southern boundary. If my understanding is correct the ocean boundary conditions taken from an ORCA12 simulation contain mesoscale features. Given that the same ocean forcing is applied at the southern (and northern) boundary for each ensemble member the same eddies (or eddy-driven features) will be felt at the southern boundary of the domain in each ensemble member in ORAC (and the other ORA\* experiments). Therefore, I expect this to lead to a signal in the South Atlantic for the ensemble mean  $\langle \text{ORAC} \rangle$ . The same does not apply in the North Atlantic as only little interannual variability seems to be imposed by the ocean conditions applied at the northern boundary. In the North Atlantic the strongest intrinsic variability originates from latitudes of about 35-40N from where coherent AMOC anomalies extend southward to the equator on interannual (or shorter) timescales (as OCAC member #2 illustrates in Figure 7). Such variability is largely filtered out in  $\langle \text{ORAC} \rangle$  as the eddy fields are decorrelated between ensemble members (and hence the timing of the interannual variability will differ). I also note here that the timing of the southern AMOC anomalies in the South Atlantic is similar between  $\langle \text{ORAC} \rangle$  and runS. This I think reinforces my point that in the South Atlantic the ocean conditions imposed at the southern boundary lead to similar timings for AMOC anomalies on interannual (and shorter) timescales.

→ Thank you for this comment. The signal imposed by our southern boundary is indeed likely to have an intrinsic origin in the global ocean. This is discussed in the paper in lines :

lines 484-491: " *In our regional configuration, this South Atlantic signal would be part of our southern boundary, and would thus emerge as a forced signal<sup>2</sup>. We have derived our open boundary conditions from the 1/12° global ocean simulation ORCA12, which is a higher resolution version of the ORAC025 configuration used by Leroux et al. (2018) in their ensemble simulations. We are thus confident that our boundary conditions are relevant for imposing a South Atlantic mode of variability.* "

The timing of this imprint is now discussed in Section 6 in response to the previous comment.

Other studies have suggested that in the South Atlantic, AMOC transport anomalies linked to eddy activity originate at about 35S from where they extend to the equator (e.g. Biastoch et al. 2008; Hirschi et al. 2013; Leroux et al. 2018). At 20S the boundary conditions from the global ORCA12 simulation will therefore likely reflect AMOC variability that originates further south.

The fact that the same ocean conditions are imposed at 20S for each ensemble member could also explain the structure of the intrinsic AMOC variability shown in Figure 6: it is largely confined to the North Atlantic reflecting that only little intrinsic variability can develop in the south Atlantic (in contrast to Biastoch et al. 2008; Hirschi et al.; Gregorio et al. 2015; and Leroux et al. 2018). Am I right that there is only little intrinsic variability in the South Atlantic in the ensemble simulations presented here?

→ Thank you for this comment. Our regional model strategy does indeed not allow us to capture the full range of intrinsic AMOC variability in the global ocean, but rather focuses on mode of variability generated within our domain, with a specific focus on the North Atlantic subtropical gyre. We have added a comment on this in Section 6:

Footnote page 23: " *Note that the forced characteristic of the imprint of the South Atlantic dynamics on the North Atlantic subtropical AMOC variability only results from our regional model strategy. It does not question the intrinsic origin of this variability in the real ocean, as proposed by others with global simulations (Biastoch et al. 2008b; Hirschi et al. 2013; Grégorio et al. 2015; Leroux et al. 2018).* "

#### Other points:

**Lines 42-44:** Note here that the examples given are not really for links between the AMOC and e.g. hurricanes and European precipitation but rather between the AMO and hurricanes/precipitation - e.g. Hallam et al. 2019 is an example where actual AMOC observations from 26N are linked to hurricane activity:

→ Thank you, we have added this additional reference.

**Lines 45-47:** I suggest to add some more references here (e.g. Menary et al. 2016, Zhang et al. 2017 ... etc)

→ Thank you, we have added this additional references.

**Lines 139-143:** Some more information about how the spinup was done would be helpful here. Is the spinup done in the following steps: 1) Spinup: 1958-1962 (starting from ORCA12 ICs) 2) IC perturbations to get states with decorrelated eddy-fields (starting dates 2 days apart in early Jan 1963) 3) Jan 1963 - Dec 1963 to ensure eddy decorrelation

→ This is correct. Further information on initial conditions and the spin-up of the model can be found in the supporting information of Jamet et al (2019). We have also added a comment on how the 5-year spin as been produces:

lines 152-153: " *The model is first spun-up for 5 years (1958-1962) from the ORCA12.L46-MJM88 initial conditions (derived from Levitus 1998 climatology) under realistic forcing.*

**Line 206:** Add reference about observations of the bottom AMOC cell e.g: Send, U., Lankhorst, M. and Kanzow, T., 2011. Observation of decadal change in the Atlantic meridional overturning circulation using 10 years of continuous transport data. *Geophysical Research Letters*, 38(24).

FrajkaWilliams, E., Cunningham, S.A., Bryden, H. and King, B.A., 2011. Variability of Antarctic bottom water at 24.5 N in the Atlantic. *Journal of Geophysical Research: Oceans*, 116(C11).

→ Thank you. Done.

**Lines 222-223; Lines 248-251** It might be useful to illustrate what the full AMOC variability looks like: e.g. standard deviation or variance for the four experiments so that we can place the leading EOF in the context of the full variability. Adding an 8th figure showing this would certainly not be a problem for the length of the paper.

→ We have included the requested figure with the associated details, and add the reference to this new figure in the discussion of EOFs:

lines 271-273: " *These differences are also seen in variance (Fig. 3), where the temporal standard deviation of the subtropical AMOC in the ensemble ORAC is about half of the standard deviation observed in the two ensembles driven by realistic atmospheric forcing.* "

**Figure 2:** The leading EOF explains 50% or less of the variance. How much variance do EOF2 and EOF3 explain? I think that it could be instructive to show EOF1 and EOF2 in Figure 2. EOF1 for experiment ORAC has a very different pattern than for

**ORAR and ORAC. I may be wrong of course but I'd suspect that EOF2 in ORAR will resemble EOF1 in ORAC.**

→ Thank you for this comment. We have mentioned in the paper the local nature of the second (and subsequent) EOFs on lines 276-278:

*"Note that we only mentioned the first EOFs here, but have also computed the second and subsequent principal components, which all exhibit more regional patterns of variability".*

However, we have not find evidence of a broad, meridionally coherent AMOC variability in the realistic ensemble ORAR which would compare to EOF1 of ensemble ORAC.

**Details:**

**As mentioned above I noted quite a few typos...etc. A few of them are listed below but there are many more so it would be desirable to carefully proof read the manuscript as part of the revision.**

→ Thank you for pointing this out, and apologies for the typos. We have corrected and performed a careful proof read of the revised version of the manuscript.

**Lines 127: insure → ensure**

**Line 134: precipitation (always singular)**

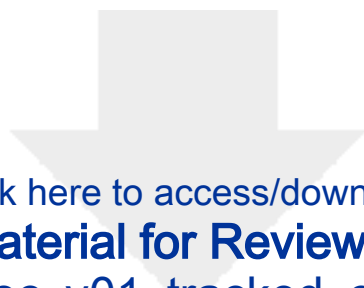
**Line 181: than → that**

**Line 182: explanations → explanations**

**Line 202: I suggest to add that "positive" means "clockwise"**

**Line 204: As above: "negative" means "anticlockwise"**

**Line 217: ... in the range of the variety... → ... in the variability range...**



[Click here to access/download](#)

**Additional Material for Reviewer Reference**  
**forced\_amoc\_v01\_tracked\_changes.pdf**

# Locally and remotely forced subtropical AMOC variability: A matter of time scales

Quentin Jamet\*

*Univ. Grenoble Alpes, CNRS, IRD, Grenoble INP, IGE, Grenoble, France*

William K. Dewar

*Univ. Grenoble Alpes, CNRS, IRD, Grenoble INP, IGE, Grenoble, France, and Dept. of EOAS,  
Florida State University, Tallahassee, FL, USA*

Nicolas Wienders

*Dept. of EOAS, Florida State University, Tallahassee, FL, USA*

Bruno Deremble

*Laboratoire de Météorologie Dynamique, Paris, France*

Sally Close

*Laboratoire d'Océanographie Physique et Spatiale, Univ. de Bretagne Occidentale, Brest, France*

Thierry Penduff

*Univ. Grenoble Alpes, CNRS, IRD, Grenoble INP, IGE, Grenoble, France*

\*Corresponding author address: Univ. Grenoble Alpes, CNRS, IRD, Grenoble INP, IGE, Grenoble,  
France

<sup>18</sup> E-mail: [quentin.jamet@univ-grenoble-alpes.fr](mailto:quentin.jamet@univ-grenoble-alpes.fr)

## ABSTRACT

19 Mechanisms driving the North Atlantic Meridional Overturning Circulation  
20 (AMOC) variability at low-frequency are of central interest for accurate cli-  
21 mate predictions. Although the subpolar gyre region has been identified as  
22 a preferred place for generating climate time scales signals, their southward  
23 propagation remains under consideration, complicating the interpretation of  
24 the observed time series provided by the RAPID-MOCHA-WBTS program.  
25 In this study, we aim at disentangling the respective contribution of the local  
26 atmospheric forcing from signals of remote origin for the subtropical low-  
27 frequency AMOC variability. We analyze for this a set of four ensembles of a  
28 regional ( $20^{\circ}\text{S}$ - $55^{\circ}\text{N}$ ), eddy-resolving ( $1/12^{\circ}$ ) North Atlantic oceanic config-  
29 uration, where surface forcing and open boundary conditions are alternatively  
30 permuted from fully varying (realistic) to yearly repeating signals. Their anal-  
31 ysis reveals predominance of local, atmospherically forced signal at interan-  
32 nual time scales (2-10 years), while signals imposed by the boundaries are  
33 responsible for the decadal (10-30 years) part of the spectrum. Due to this  
34 marked time scale separation, we show that, although the intergyre region  
35 exhibits peculiarities, most of the subtropical AMOC variability can be un-  
36 derstood as a linear superposition of these two signals. Finally, we find that  
37 the decadal scale, boundary forced AMOC variability has both northern and  
38 southern origin, although the former dominates over the latter, including at  
39 the site of the RAPID array ( $26.5^{\circ}\text{N}$ ).

## 40 **1. Introduction**

41 The Atlantic Meridional Overturning Circulation (AMOC) plays a central role in climate by  
42 redistributing heat, freshwater and carbon. Its strength is correlated with climate indices such as  
43 the Atlantic Multidecadal Variability (AMV, Kushnir 1994; Schlesinger and Ramankutty 1994;  
44 Kerr 2000), (Knight et al. 2005; McCarthy et al. 2015b), as well as to the occurrence of regional  
45 weather events. Examples are precipitations over Europe (Sutton and Dong 2012) and North  
46 Africa (Zhang and Delworth 2006) and the hurricane activity in North America (Goldenberg et al.  
47 2001; Hallam et al. 2019). Thus, understanding the mechanisms pacing AMOC variability at  
48 climate time scales is of central interest for climate predictions. Decadal AMOC variability is  
49 often argued to be paced by the North Atlantic subpolar gyre due to the longer time scales involved  
50 in its dynamics (Wunsch and Heimbach 2013; Menary et al. 2016; Zhang 2017). But subpolar-  
51 subtropical AMOC connectivity remains an open question, with potentially complex interactions  
52 between the Deep Western Boundary Current (DWBC) and the upper Gulf Stream. Placing the  
53 focus on the subtropical gyre where continuous measurements of the AMOC have been carried out  
54 since 2004 by the RAPID-MOCHA-WBTS program (McCarthy et al. 2015a), we wish to further  
55 categorize the low-frequency AMOC variability of this region as locally or remotely paced.

56 A prevailing concern regarding mechanisms driving the low-frequency AMOC variability in  
57 the subtropical gyre is associated with the southward propagation of density anomalies from the  
58 subpolar gyre. While the subtropical gyre is dominated by interannual AMOC variability, the  
59 subpolar gyre is dominated by decadal time scales dynamics (Balmaseda et al. 2007; Wunsch  
60 2013; Wunsch and Heimbach 2013), such as deep water formation rates or the longer time it  
61 takes for baroclinic Rossby waves to cross the basin at higher latitudes (Wunsch and Heimbach  
62 2013). This makes the subpolar gyre a preferred region for the generation of decadal time scales

63 signals. Of particular importance is the southward propagation of dense water masses, which  
64 are expected to propagate to the subtropical gyre through the DWBC. As nicely reviewed by  
65 Biastoch et al. (2008a), mechanisms involved in the southward propagation of signals within the  
66 DWBC include a rapid exit of newly generated deep water masses out of the subpolar gyre and  
67 a fast equatorward communication through coastal Kelvin waves (Kawase 1987; Johnson and  
68 Marshall 2002; Deshayes and Frankignoul 2005; Hodson and Sutton 2012). Those southward  
69 traveling coastally trapped density anomalies thus lead to a zonal gradient across the North Atlantic  
70 basin, pacing an AMOC variability through geostrophic adjustment (Hirschi and Marotzke 2007;  
71 Cabanes et al. 2008; Tulloch and Marshall 2012; Buckley et al. 2012; Jamet et al. 2016).

72 However, recent studies cast doubt on such a simple southward pathway of density anomalies  
73 from the subpolar to the subtropical gyre. Observations do not reveal a straightforward connec-  
74 tion between deep water masses production at high latitude and their export further south (Schott  
75 et al. 2004; Lozier 2010). Both observational (Bower et al. 2009) and numerical (Zou and Lozier  
76 2016) float experiments suggest rather that recently formed deep water masses in the Labrador Sea  
77 mainly recirculate within the subpolar gyre, and that only a small fraction transit further south, a  
78 dynamics recently supported by the first 21 months of the OSNAP observing system (Lozier et al.  
79 2019). Additionally, a few studies have highlighted the complex dynamics involved in the south-  
80 ward propagation of the DWBC when crossing the upper, northward flowing Gulf Stream, with  
81 strong vertical interactions (Spall 1996a,b; Bower and Hunt 2000; Zhang and Vallis 2007; Andres  
82 et al. 2016).

83 Regarding southern interactions, Biastoch et al. (2008b) highlighted the potential contribution  
84 of the Agulhas linkage for the AMOC variability in the North Atlantic subtropical gyre. Using  
85 a two-way nested global configuration with refined horizontal resolution in the Agulhas region,  
86 they show that the meso-scale dynamics of this region contributes to about 0.2 Sv ( $1 \text{ Sv} = 10^6 \text{ m}^3$

87  $s^{-1}$ ) of the lower limb AMOC decadal variability, which may well contribute to about 10-20%  
88 of the  $\sim O(1 \text{ Sv})$  low-frequency variability measured by the RAPID array (Smeed et al. 2014,  
89 2018). Such a potential contribution of the southern Atlantic for the AMOC variability in the  
90 North Atlantic subtropical gyre has also been recently underscored by Leroux et al. (2018).

91 AMOC variability in the subtropical gyre also responds to the local atmospheric forcing. On  
92 short time scales (month-to-years), the Ekman adjustment of the ocean to local wind stress has  
93 been proposed as the leading mechanism (Hirschi and Marotzke 2007). At longer time scales,  
94 the baroclinic shear adjustment and the gyre interaction with an irregular bathymetry dominates  
95 (Häkkinen 2001; Cabanes et al. 2008). Thus, a measure of the AMOC as provided by the RAPID  
96 array would likely be a potentially complex combination of signals of different origin. Through  
97 numerical sensitivity experiments to surface forcing, Biastoch et al. (2008a) however have shown  
98 that the variability of the maximum AMOC under realistic forcing can be understood as a linear  
99 combination of an interannual variability driven by local wind forcing, and a decadal variability  
100 driven by buoyancy forcing in the Labrador Sea. This linear superposition has also been under-  
101 scored recently by Kostov et al. (Sub.) in the ECCO state estimate through adjoint sensitivity  
102 experiments to ocean surface metrics, with a leading role of zonal wind stress in the local re-  
103 sponse. This would suggest that interactions between the ocean response to the local atmospheric  
104 forcing and signals of remote origin are weak, making attribution in the real ocean easier. But  
105 these studies have also pointed out the potential sensitivity of this linear superposition to the pres-  
106 ence of oceanic eddies. We thus propose here to further analyze this linear superposition in such  
107 an eddying regime.

108 To further disentangling the respective contribution of the local atmospheric forcing for the  
109 AMOC variability in the North Atlantic subtropical gyre from the signals generated in remote  
110 regions (such as North Atlantic subpolar or Agulhas regions), we analyze the model outputs of 4

different regional ocean model configurations which differ in their forcing at the surface and at the open boundaries. Details of these simulations are given in Section 2. In order to explicitly resolve the oceanic meso-scale dynamics (important for many oceanic processes, and in particular involved in the evolution of water mass properties in the DWBC downstream of Grand Bank (Bower and Hunt 2000; Lozier 2010)), we have performed these simulations at eddy-resolving ( $1/12^\circ$ ) horizontal resolution. With such a resolution, a significant fraction of the AMOC variability is expected to be intrinsic, that is, driven by processes other than the forcing and with a random phase (Hirschi et al. 2013; Grégorio et al. 2015; Leroux et al. 2018; Jamet et al. 2019b). We have thus carried out these simulations with an ensemble strategy. We discuss in the following the results of the ensemble mean, which reflects the oceanic response to external forcing (surface and boundaries). We first extract the leading modes of the forced AMOC variability in our four ensembles, and compare their spatial pattern and their spectral content (Section 3). We then analyze full time series to assess the assumption of linearity in the combined effect of surface and boundary forced signals, and we illustrate the benefits of our ensemble strategy to identify AMOC responses to external forcing in an eddying ocean (Section 4). We discuss the intrinsic AMOC variability simulated by our different ensembles in Section 5, and analyze the respective contribution of northern and southern open boundaries for driving boundary forced AMOC variability in Section 6. We summarize and discuss our results in Section 7.

## 2. Methods

### *a. Model, experiments and processing*

We use the regional North Atlantic configuration of the Massachusetts Institute of Technology General Circulation Model (MITgcm, Marshall et al. 1997) described in Jamet et al. (2019b). It

133 extends from 20°S to 55°N with a horizontal resolution of 1/12° and 46 layers in the vertical, rang-  
134 ing from 6 m at the surface to 250 m at depth. Open boundary conditions are applied at the side of  
135 our domain, such that oceanic velocities (U, V) and tracers (T, S) are restored with a 36 minutes  
136 relaxation time scale toward oceanic state derived from the 55-year long 1/12° horizontal resolu-  
137 tion ocean-only global NEMO simulation ORCA12.L46-MJM88 (Molines et al. 2014). To insure  
138 stability at the boundary, a sponge layer is applied to the two adjacent grid points where model  
139 variables are restored toward boundary conditions with a 1 day relaxation time scale. Although  
140 these relaxation times scales are relatively short, no adverse effects were apparent upon inspection.  
141 Open boundary conditions are applied every 5 days and linearly interpolated in between.

142 At the surface, the ocean model is coupled to an atmospheric boundary layer model (CheapAML,  
143 Deremble et al. 2013). In CheapAML, atmospheric surface temperature and relative humidity re-  
144 spond to ocean surface structures by exchanges computed according to the COARE3 (Fairall et al.  
145 2003) flux formula, but are strongly restored toward prescribed values over land. Other vari-  
146 ables (downward longwave and solar shortwave radiations, precipitations) are prescribed every-  
147 where. Atmospheric reanalysis products used in CheapAML originate from the Drakkar forcing  
148 set (DFS4.4, Brodeau et al. 2010; Dussin et al. 2016), consistent with the atmospheric forcing  
149 employed in the ORCA12.L46-MJM88 global simulation used to derive the open boundary con-  
150 ditions.

151 The model is first spun-up for 5 years (1958-1962) from the ORCA12.L46-MJM88 initial con-  
152 ditions (derived from Levitus 1998 climatology) under realistic forcing. Then, all ensembles are  
153 integrated forward in time for 50 years (1963-2012) with a 12-member ensemble strategy. The  
154 12 initial conditions have been constructed through 1-year long simulations under 1963 forcing  
155 initialized with 2-day apart ocean states from January, 1963. These initial conditions are meant  
156 to reflect the spread induced by the growth of small, dynamically consistent perturbations decor-

related at seasonal time scales. This set of 12 initial conditions is used across the four different ensembles, such that initial perturbations are the same in all experiments. Further details on the configuration can be found in (Jamet et al. 2019b, Supporting Information). We focus here our analysis on the ensemble mean statistics, which we interpret as the oceanic response to external forcing (surface and boundaries). This ensemble means are thus referred to as the forced variability in the following. The departure from this ensemble mean, i.e. the ensemble spread due to intrinsic variability, is discussed in Section 5.

To disentangle the respective contribution of open boundaries and surface forcing in driving oceanic variability within our regional North Atlantic domain, we have alternatively permuted open boundaries and surface forcing from fully varying (realistic) to yearly repeating signals. The realistic ensemble (referred to as ORAR hereafter, for Open boundary conditions Real and Atmosphere Real) uses the full spectrum of open boundary conditions and surface forcing. This ensemble represents the reference test case associated with realistic conditions, which has been used by Jamet et al. (2019b) to separate forced and intrinsic AMOC variability. Results from the three other ensembles are compared to this reference experiment. To isolate the oceanic variability that is locally forced by the interannual-to-decadal atmospheric dynamics, climatological open boundary conditions are applied to the ensemble OCAR (Open boundary conditions Climatologic and Atmosphere Real). These climatological open boundary conditions have been constructed as a climatological average for the period 1963-2012, i.e. 5-day open boundary conditions are averaged across the years to provide a mean representation of the seasonal cycle. They repeat every year, such that no signals at interannual and longer time scales are imposed by the boundaries. By contrast, to isolate the imprint of open boundaries, yearly repeating atmospheric forcing is applied to the ensemble ORAC (Open boundary conditions Real and Atmosphere Climatologic). The yearly repeating atmospheric forcing follows a 'normal' year strategy (Large and Yeager 2004). This

choice emerged from the recognition that, when using CheapAML, transient atmospheric winds need to be accounted for to simulate a realistic oceanic mean state (Jamet et al. 2019). These are absent from climatological atmospheric conditions. The period August 2003 to July 2004 has been selected because it minimizes the difference between the number of occurrences of the Atlantic Ridge weather regime and its 1958-2012 climatological mean. We have placed the focus on the Atlantic Ridge weather regime to identify a normal year since it has been shown to be the weather regime the most correlated to the North Atlantic subtropical Sea Surface Height interannual variability (Barrier et al. 2013). The occurrence of this weather regime has been found to induce a northward shift of the wind-stress curl, altering the Sverdrup balance and generating westward propagating Rossby waves. Such processes are of importance for the low-frequency variability of the North Atlantic large-scale circulation such as the Atlantic Meridional Overturning Circulation (AMOC) which is closely linked to the intensity of the gyres (Zhang 2008). A fourth ensemble (OCAC, Open boundary conditions Climatologic and Atmosphere Climatologic) is run with both climatological boundary conditions and 'normal' year atmospheric forcing, such that the forcing involves no frequencies longer than one year. This fourth ensemble provides us a quantitative estimate of the AMOC variability that we cannot interpret as forced by the low-frequency variability of the atmospheric forcing or the boundary conditions. Although not exhaustive, possible explanations for the presence of a low-frequency, ensemble mean AMOC variability in this ensemble may involve the presence of a 'residual' intrinsic variability due to the size of our ensemble (12 members), or the development of a forced low-frequency AMOC variability through non-linear processes. Such questions are however out of the scope of this paper, and thus left for further studies.

Finally, two additional single simulations (with no ensemble strategy) are run with fully varying open boundary conditions only at the southern or the northern extend of the domain, while all

other forcing (including the surface) are yearly repeating. These two simulations will be used in Section 6 to disentangle the respective contribution of the northern and the southern boundary for generating boundary forced AMOC variability in the subtropical gyre. Table 1 provides a summary of the simulations discussed in this study.

Our focus is placed on interannual-to-decadal AMOC variability. The model output 5-day averaged AMOC time series are thus band-pass filtered to remove large variance at sub-annual time scales, trends and very long frequencies unresolved by our 50-year long simulations. The filter is a combination of high- and low-pass filters, and a seasonally varying climatological mean is removed. This time filtering isolates periods between 2 and 30 years (Jamet et al. 2019b). First and last years of simulations are discarded in the following analyses due to side effects of this time filtering.

## *b. Mean state*

The time mean overturning circulation (computed in depth space) simulated by our reference, realistic ensemble (ORAR; Fig. 1, top left panel) exhibits a positive cell in the 3000 upper meters, peaking at about 18 Sv ( $1 \text{ Sv} = 10^6 \text{ m}^3 \text{ s}^{-1}$ ) at  $34^\circ\text{N}$  and 1200 m depth. Below 3000 m the overturning streamfunction is negative and of about 4-5 Sv at 4000 m depth. Near the surface, we also note the presence of two shallow subtropical wind-driven cells in the upper 200 m. Although the bottom negative cell is slightly stronger than in observations (Send et al. 2011; Frajka-Williams et al. 2011), all these features are typical of what is usually found in ocean-only (Danabasoglu et al. 2014) and climate models (Gastineau and Frankignoul 2012; Muir and Fedorov 2016). Further comparisons of the ensemble mean AMOC and the RAPID-MOCHA-WBTS observational estimates can be found in the Supporting Information of Jamet et al. (2019b).

227 The three remaining panels of Fig. 1 provide estimates of the modified mean state when forcing  
 228 (surface and open boundaries) is turned to yearly repeating signals. The time mean AMOC is  
 229 reduced by about 0.1-0.2 Sv in most of the basin under climatological open boundary conditions,  
 230 with the largest reduction observed near the AMOC time mean maximum, i.e. 34°N and 1200 m  
 231 depth (top right panel). The effects of turning the atmosphere from realistic to yearly repeating  
 232 forcing is, not surprisingly, most pronounced in the upper layers, with notably a weakening of  
 233 the northern hemisphere subtropical wind-driven cell by about -2 Sv (bottom left panel). Time  
 234 mean AMOC changes are otherwise mostly positive with local maximum ( $\sim 0.5$  Sv) in localized  
 235 regions. The OCAC ensemble time mean AMOC changes illustrate the combination of these two  
 236 effects (bottom right panel). Overall, those changes remain weak in amplitude and thus lie in the  
 237 range of the variety of time mean AMOC usually simulated by models. Thus, as we will discuss  
 238 below, changes in the forcing at the surface and at the boundaries primarily impact the simulated  
 239 low-frequency AMOC variability, with little changes in the time mean AMOC state on which this  
 240 variability develops.

### 241 **3. Leading modes of forced AMOC variability**

242 We extract the leading modes of forced AMOC variability in each ensemble by performing a  
 243 Principal Component Analysis (PCA) on the ensemble mean AMOC (Fig. 2). The EOF1 of the  
 244 reference, realistic ensemble (ORAR, top left panel) exhibits a broad positive signal over most of  
 245 the domain, peaking to about 1.2 Sv at 15°N and 1500 m depth, and a sign reversal around 45°N  
 246 and 15°S. It explains slightly less than 40% of variance, and has been interpreted, in connection  
 247 with previous studies, as the AMOC response to yearly varying atmospheric forcing by Jamet  
 248 et al. (2019b). This interpretation is further supported here by comparing this leading mode of  
 249 AMOC variability under realistic forcing against those obtained in the other ensembles. When the

interannual and longer variability of the atmosphere is removed and the surface forcing repeats  
 every year (ORAC, bottom left panel), the spatial pattern of the leading mode radically changes.  
 It now exhibits a large band of meridionally coherent AMOC anomalies with no sign reversal,  
 revealing the imprint of remotely-forced signals on the subtropical AMOC variability. It reaches  
 its maximum near the maximum of the time mean AMOC, i.e. at 1200 m depth. We note here that  
 the meridional structure of this mode indicates a tendency of the AMOC to oscillate in phase at all  
 latitudes. This would thus suggest a rapid communication of boundary signals toward the interior  
 of the domain, potentially through Kelvin waves as suggested by others (Johnson and Marshall  
 2002; Biastoch et al. 2008b; Zhang 2010; Hodson and Sutton 2012; Leroux et al. 2018). In con-  
 trast, when the imprint of the low-frequency atmospheric forcing on AMOC variability is isolated  
 from the influence of the boundaries (OCAR, top right panel), the leading mode of variability is  
 found to be similar to the one obtained under realistic forcing, i.e. a 'gyre-specific' mode with  
 a sign reversal at the intergyre. Comparing the results of these two ensembles (i.e. ORAC and  
 OCAR) with those obtained under realistic forcing (i.e. ORAR) strongly supports earlier interpre-  
 tations: The leading mode of the forced AMOC variability extracted through a PCA on a realistic  
 simulation reflects the oceanic response to the local atmospheric forcing (Eden and Jung 2001;  
 Eden and Willebrand 2001; Deshayes and Frankignoul 2008; Gastineau and Frankignoul 2012;  
 Jamet et al. 2019b). Such an interpretation is also consistent with the relative magnitude of these  
 modes. Although they all explain about 40 to 50% of the forced AMOC variability, the leading  
 mode in the ensemble ORAC is weaker ( $\sim 0.4$ - $0.5$  Sv) compared to those obtained under realis-  
 tic atmospheric forcing ( $\sim 1$  Sv). These differences are also seen in variance (Fig. 3), where the  
 temporal standard deviation of the subtropical AMOC in the ensemble ORAC is about half of the  
 standard deviation observed in the two ensembles driven by realistic atmospheric forcing. Thus,  
 due to the stronger signal imprinted by the local, low-frequency atmospheric forcing on the ocean

274 circulation, these dynamics are naturally identified as leading modes of variability through a PCA  
275 since the latter looks for modes with the largest variance. Note that we only mentioned the first  
276 EOFs here, but have also computed the second and subsequent principal components, which all  
277 exhibit more regional patterns of variability.

278 When both surface and open boundary forcing are yearly repeating (ensemble OCAC), a weak  
279 'residual' variability appears. The PCA of this 'residual' variability reveals that about 35% of  
280 this variability is characterized by a large scale mode that strongly resembles the intrinsic mode  
281 of AMOC variability identified by Jamet et al. (2019b) in the realistic (ORAR) ensemble, and  
282 discussed in Section 5. This suggests this mode of 'forced' variability is likely to reflect a remnant  
283 of the intrinsic variability due to the relatively modest size of our ensemble size, i.e. 12 members.  
284 Although not conclusive, this supports our interpretation of a quantitative estimate of the AMOC  
285 variability that cannot be interpreted as forced by the low-frequency variability of the forcing.

286 Aside from their differences in spatial patterns, these modes also exhibit very distinct spectral  
287 contents. We illustrate this in Fig. 4 by reconstructing the time series of their respective maximum,  
288 i.e. multiplying the normalized PCs by the local maximum of their associated EOFs. The aim of  
289 this reconstruction is to simplify the interpretation, where spectral properties of these modes are  
290 shown with their respective amplitude. From their time series, it is clear that the leading mode  
291 of forced AMOC variability in the ensembles ORAR and OCAR (both driven by realistic atmo-  
292 spheric forcing) vary almost perfectly in phase. Their respective Power Spectral Density (PSD)  
293 functions confirm such an agreement in term of spectral content. The agreement is particularly  
294 pronounced at interannual time scales, where both of these modes exhibit two local maximum at  
295 2-3 and 6-8 years frequency bands typical of the North Atlantic atmospheric spectrum (Czaja and  
296 Marshall 2001; Reintges et al. 2017). When the ocean is driven by a yearly repeating atmospheric  
297 forcing however (ORAC and OCAC ensembles), the interannual variance strongly reduces and

most of the energy resides at decadal time scales. The ensemble driven by fully varying open boundary conditions (ORAC) exhibits indeed a large peak of variability in the 10-30 years band, which exceeds the spectral energy of the leading mode obtained in the realistic (ORAR) ensemble. This result further supports our earlier interpretation that the leading mode of AMOC variability computed under realistic conditions reflects the response to a local, low-frequency atmospheric forcing, but contains little information about the boundary forced signal.

The PCA discussed here provides a statistical description of the main spatio-temporal patterns of AMOC variability. It however only accounts for a given fraction (about 40-50% in our ensembles) of the total signal. We thus extend our spectral analysis in the following by considering full time series to further investigate time scale separation between local atmospherically forced and remotely forced AMOC variability, and assess their linear combination for interpreting realistic time series.

## 4. Testing the linear combination assumption

### *a. Analysis of full time series*

We now wish to extend our results to full time series in order to account for the complete low-frequency AMOC spectrum. To replace our numerical results in an observational context, we choose to look first at the time series simulated by our four ensembles at 26.5°N, that is, the latitude of the RAPID-MOCHA-WBTS array (McCarthy et al. 2015a). AMOC time series at that location are plotted on the top left panel of Fig. 5, and their associated PSDs appear on the top right panel <sup>1</sup>.

---

<sup>1</sup>For comparison, the 1-year low-pass filtered RAPID array time series is shown in purple on the top left panel. Note however that a direct comparison with the ensemble mean AMOC time series is not possible due to the presence of intrinsic AMOC signals in the RAPID time series.

318 Differences in the AMOC time series of our ensembles are largest between the two ensembles  
319 driven by the full spectrum of atmospheric forcing, i.e. ORAR and OCAR, against those driven  
320 by yearly repeating atmospheric forcing, i.e. ORAC and OCAC, reflecting here again the stronger  
321 control of the local atmospheric forcing on the low-frequency AMOC variability. Thus, AMOC  
322 variability simulated by the ensemble OCAR tends to closely follow that simulated by the realistic  
323 ensemble ORAR, with most of the interannual peaks of variability consistently reproduced. We  
324 note for instance that the several Sverdrup downturn in 2009-2010, which has been monitored  
325 by the RAPID array and interpreted as an atmospherically forced signal (Roberts et al. 2013;  
326 Zhao and Johns 2014; Leroux et al. 2018), is well reproduced by the two ensembles driven by  
327 fully varying atmospheric forcing, but is not in the two ensembles driven by yearly repeating  
328 atmospheric forcing. Our results are thus consistent, and support, this earlier interpretation. We  
329 note however that the ensemble OCAR exhibits a more energetic AMOC variability in the 3-6 year  
330 band than the realistic ensemble ORAR (top right panel). This would suggest that low-frequency  
331 atmospheric forcing drives an AMOC variability within this frequency band which is damped by  
332 the realistic open boundary forcing.

333 Focusing now on decadal time scales, spectral analysis reveals that the AMOC variability in the  
334 ensemble OCAR is weak compared to the realistic ensemble ORAR (Fig. 5, top panels). Results  
335 from the ensemble ORAC suggest that the spectral content of the AMOC variability at those time  
336 scales is indeed driven by the open boundaries, with a spectral content consistently reproduced.  
337 These results thus suggest that the time scale separation between the local, atmospherically forced  
338 signal and the signal driven by open boundaries identified for leading EOFs holds for the full time  
339 series of AMOC variability. As a result, it is likely that the subtropical AMOC variability could

---

These intrinsic signals have been estimated to account for about 0.9 Sv at RAPID site (Jamet et al. 2019b), thus contributing significantly to the mismatch between the RAPID time series and the ensemble mean AMOCs.

be understood as a linear superposition of these two signals. We will further test this assumption in Section 4b.

We now wish to extend these results to all latitudes in our domain, that is, from 20°S to 55°N. At 1200 m depth, the maximum of the time mean AMOC, we then compute at all latitudes the PSD function of AMOC time series for each ensemble mean, and compare their results. Results appear on Fig. 6 for the three ensembles ORAR, OCAR and ORAC. Results for the ensemble OCAC are not shown. Previous analyses show a very weak signal in this ensemble, and we have verified that this holds at all latitudes. Results from the ensemble ORAC confirm our earlier findings, that is, the open boundary conditions drive AMOC variability at decadal time scales. For shorter time scales, the spectral content in this ensemble is weak and do not explain any of the spectral peaks in the 1-10 year band found in the realistic ensemble ORAR. Similarly, results from the ensemble OCAR confirm that the local atmospheric forcing drives AMOC variability at interannual time scales. In this frequency band, the spectral content of the realistic ensemble ORAR is consistently reproduced. However, we found that the ensemble OCAR also exhibits significant AMOC variability at decadal time scales in the 30-40° latitude band. This would suggest that at these latitudes the atmosphere exerts a stronger effect on decadal AMOC variability. This region is characterized by the subpolar-subtropical intergyre position, suggesting a potential adjustment of the latter to decadal fluctuation in the local wind stress (Zhang 2010). At these latitudes, both remote signals and local atmospheric forcing imprint a decadal AMOC variability, with potentially complex interactions.

To conclude, although peculiarities arise at the subpolar-subtropical intergyre position (30-40°N), spectral estimates highlight that forced AMOC variability is driven by local atmospheric forcing at interannual time scales and remote processes at decadal time scales in most of the subtropical gyre. Based on this time scale separation, we thus suspect that in the realistic ensemble

364 ORAR, AMOC variability can be understood as a linear combination of these two sources of  
365 variability as suggested earlier by Biastoch et al. (2008a).

366 *b. The linear assumption*

367 We aim here at assessing to which extent the realistic forced AMOC variability can be under-  
368 stood as a linear combination of local, atmospherically forced and remotely generated signals.  
369 For this purpose, we reconstruct an AMOC streamfunction as the sum of the two streamfunctions  
370 simulated by the ensembles OCAR and ORAC, and compare it with the realistic ensemble ORAR.  
371 Following the previous section, we first present and discuss results at  $26.5^{\circ}\text{N}$ , and then extend our  
372 analysis at all latitudes of our regional domain.

373 At  $26.5^{\circ}\text{N}$  (Fig. 5, bottom panels), results from this reconstruction are promising. The recon-  
374 structed time series is highly correlated ( $r = 0.9$ ) to the realistic forced AMOC variability, and  
375 lies within the ensemble spread induced by intrinsic ocean dynamics (gray shading). When taken  
376 separately, the forced AMOC variability in the ensemble OCAR (ORAC) is correlated to  $r = 0.8$   
377 ( $r = 0.3$ ) to the time series diagnosed in the realistic ensemble ORAR. Added together, the contri-  
378 bution of each ensemble dynamics is to improve correlation with realistic estimates of the forced  
379 AMOC variability, although most of the correlation is due to the atmospheric forcing, consistent  
380 with a stronger control of the latter compared to remote signals. The large strengthening of the  
381 AMOC by about 4 Sv in the mid-1990s provides a nice illustration for this reconstruction. Over  
382 this period, the AMOC time series in the ensemble OCAR is indeed off by about 1 Sv compared to  
383 the realistic ensemble ORAR. But the ensemble ORAC exhibits at the same time a low-frequency  
384 signal that contributes to about 1 Sv to the strengthening of the AMOC. Added together, the recon-  
385 structed time series is in very good agreement with the AMOC variability in realistic conditions  
386 over that period.

387 Although the correlation between the two time series is high ( $r = 0.9$ ), we note however that  
388 differences occur over the course of the simulation. Spectral analyses highlight that such discrep-  
389 ancies have preferred frequency, with a more energetic reconstructed AMOC in the 3-6 year band  
390 and at decadal time scales (Fig. 5, bottom right panel). The 3-6 year band corresponds to the fre-  
391 quency band where the ensemble OCAR exhibits an over estimated AMOC variability compared  
392 to the realistic scenario (cf Section 4a). These results would suggest that in this frequency band,  
393 the AMOC variability at  $26.5^\circ\text{N}$  cannot be understood as a linear combination of two independent  
394 signals, but rather that the interactions between them needs to be accounted for.

395 We now extend the analysis of the reconstructed AMOC time series for all range of latitude  
396 within our domain. At 1200 m depth, the spectral content of the reconstructed AMOC super-  
397 imposes on the spectral content of the realistic ensemble ORAR with a good level of agreement  
398 (Fig. 6). The general patterns of the spectral content closely match, and regions of high spectral  
399 density are consistently reconstructed. This visual inspection is further supported by taking the  
400 difference of these two PSDs. Results appear on the bottom right panel of Fig. 6, where blue col-  
401 ors indicate a more energetic reconstructed AMOC. Although significant differences are observed  
402 at specific locations, we found that most of the AMOC variability in our realistic ensemble can be  
403 understood as a linear combination of the two ensembles OCAR and ORAC. Marked differences  
404 appear however at some localized spots, such as the decadal AMOC variability in the  $30\text{-}40^\circ\text{N}$   
405 latitude band. We identified earlier this latitude band as a region where the local atmospheric  
406 forcing imprints an AMOC variability at decadal time scales. Such a surface forcing would thus  
407 potentially interact with the decadal signal imposed by the boundaries, leading to a more complex  
408 signal than a simple linear combination. We also note that the mismatch in the 3-6 year band  
409 between the reconstructed and the realistic AMOC variability at  $26.5^\circ\text{N}$  seems to be a peculiarity  
410 of the  $20\text{-}30^\circ\text{N}$  latitude band.

411     Permuting open boundaries and surface forcing from realistic to yearly repeating signals induces  
 412     an imbalance between the state of the ocean and the applied new boundary conditions. To adjust,  
 413     the ocean is likely to generate wave-like signals in response to these changes, such that we cannot  
 414     exclude the presence of artificial modes in our regional configuration. Such modes could imprint  
 415     into the AMOC, and may well play a role in the overestimated variability at 26.5°N and in the 30-  
 416     40°N latitude band diagnosed in the ensemble OCAR. Although further analyses are required to  
 417     consistently assess the potential effects of such modes, we note that our results are similar to what  
 418     Leroux et al. (2018) diagnosed in their global and North Atlantic  $\frac{1}{4}^\circ$  ensembles. When constrained  
 419     by imposed climatological boundary conditions at 21°S and 81°N, the two leading modes of the  
 420     ensemble mean AMOC in their 10-member regional North Atlantic ensemble exhibit a slightly  
 421     larger amplitude than the leading modes diagnosed in their global, 50-member ensemble. The two  
 422     ensembles used by Leroux et al. (2018) are significantly different from ours, especially regarding  
 423     boundary conditions, but they exhibit differences that compare well with our results. This suggests  
 424     a dynamical origin of the overestimated AMOC variability in our OCAR ensemble rather than  
 425     numerical artifacts.

### 426     *c. Benefits of the ensemble*

427     We have shown that the realistic AMOC variability within the North Atlantic subtropical gyre  
 428     can be understood, to a good extent, as a linear superposition of signals with different origins.  
 429     This supports the earlier findings of Biastoch et al. (2008a) and Kostov et al. (Sub.), and extends  
 430     their results in an eddying regime. We recall that we have performed our analysis with an ensemble  
 431     strategy, which we want to illustrate the benefits to identify the ocean responses to external forcing.  
 432     We compare here the results of our ensemble analysis with results one could obtain with single  
 433     simulations. The four ensembles have been initialized with the same set of 12 initial conditions.

434 Comparing the members across the ensembles is thus the analog of regular sensitivity experiments  
435 conducted with single simulations, i.e. with no ensemble strategy.

436 We consider here the correlation between the reconstructed and the realistic AMOC variability.  
437 Results appear on the left panel of Fig. 7 for the reconstruction based on ensemble means. The  
438 reconstructed AMOC is correlated to the realistic AMOC to at least  $r = 0.9$  in most of the basin.  
439 These correlations weakened in the Gulf Stream region and at depth, where intrinsic AMOC vari-  
440 ability has been shown to be the largest (Jamet et al. 2019b). When considering only one member  
441 however (Fig. 7, middle panel), the correlations strongly reduce in most of the basin. At 1200 m  
442 depth (right panel), correlations drops to  $r = 0.6$  in the subtropical gyre and to  $r = 0.2$  in the Gulf  
443 Stream region. These low correlations reflect the presence of an intrinsic AMOC variability which  
444 we further discuss in Section 5. This intrinsic AMOC variability imprints in all simulations with  
445 similar patterns and spectral contents, but with a random phase. These contributions do not add  
446 linearly, explaining the lower correlations obtained when considering single, eddy-resolving sim-  
447 ulations. This result illustrates the benefits of ensemble simulations to disentangle the respective  
448 role of the forcing in eddy-resolving simulations, where intrinsic ocean variability that emerge at  
449 these resolutions needs to be filtered.

## 450 **5. Intrinsic AMOC variability**

451 We have thus far focused on the forced AMOC variability as simulated by our four ensembles.  
452 This forced signal has been computed through an ensemble average. This averaging operation  
453 captures the signal common to all members within an ensemble, and thus reflects the ocean re-  
454 sponse to external forcing (we recall here that all members of an ensemble are exposed to the  
455 same surface and open boundary forcing). However, each member within a given ensemble is not  
456 locked to this ensemble mean. They exhibit sensitivity to initial conditions such that a significant

457 portion of the AMOC variability within a given member is driven by intrinsic oceanic dynamics  
458 (Hirschi et al. 2013; Grégorio et al. 2015; Leroux et al. 2018; Jamet et al. 2019b). We thus now  
459 want to focus on this intrinsic component of the variability by considering the ensemble spread in  
460 our four ensembles and assess its sensitivity to changes in the forced signal.

461 Following Jamet et al. (2019b), we first compute, within each of the four ensembles, the de-  
462 parture of each member from its associated ensemble mean. We then perform a PCA on each  
463 ensemble member residual and average the results together to yield a map of intrinsic AMOC  
464 variability. Results of this analysis highlight the presence of a basin scale mode of intrinsic vari-  
465 ability in each ensemble that strongly resembles the intrinsic basin scale mode identified by Jamet  
466 et al. (2019b) in the realistic ensemble ORAR (Fig. 8). This basin scale mode peaks at about 1.2  
467 Sv in the subtropical gyre near 2000 m depth, and mostly expresses at interannual time scales.  
468 In previous sections, we have discussed the fundamentally different characteristics of the forced  
469 AMOC variability simulated by these ensembles. Thus, the level of agreement found in the intrinsic  
470 component of these ensembles highlights the very weak sensitivity of the basin scale mode of  
471 intrinsic AMOC variability to changes in the surrounding forced component of the AMOC vari-  
472 ability. Such a weak sensitivity has been reported earlier by Leroux et al. (2018) for the intrinsic  
473 AMOC variability at mid-depth. Our results provide a vertical and spectral generalization of this  
474 earlier finding.

## 475 **6. Northern and southern origin of the decadal AMOC variability**

476 Biastoch et al. (2008b) have provided evidence that decadal AMOC variability in the North  
477 Atlantic subtropical gyre might be imprinted by Agulhas meso-scale dynamics. Those results  
478 contrast with the prevailing mechanism for explaining the decadal subtropical AMOC variability  
479 as being paced by high latitude processes such as deep water formation. Their results have re-

cently been supported by Leroux et al. (2018) in their 50-member global ocean ensemble, where they identified a South Atlantic mode of intrinsic AMOC variability. This suggests that the meso-scale dynamics of the Agulhas current has the potential to pace intrinsic AMOC variability further north, and thus are likely to imprint on the RAPID observations at  $26.5^{\circ}\text{N}$ . In our regional configuration, this South Atlantic signal would be part of our southern boundary, and would thus emerge as a forced signal<sup>2</sup>. We have derived our open boundary conditions from the  $1/12^{\circ}$  global ocean simulation ORCA12, which is a higher resolution version of the ORCA025 configuration used by Leroux et al. (2018) in their ensemble simulations. We are thus confident that our boundary conditions are relevant for imposing a South Atlantic mode of variability. To isolate the influence of our southern boundary from its northern counterpart, we analyze the two additional simulations runN and runS driven by either northern or southern fully varying boundary conditions, the remaining forcing being yearly repeating (including surface forcing).

Due to large computational time required to generate ensembles, we were not able to produce ensembles for these additional simulations. They are thus single realizations, such that ensemble statistics are not at our disposal for accurately separating the forced AMOC variability from its intrinsic counterpart. Instead, we leverage results from our four ensembles to interpret the dynamics simulated by these two additional single simulations. We particularly recognize that those two simulations are driven with yearly repeating atmospheric forcing, such that interannual forced AMOC variability in the North Atlantic subtropical gyre is expected to be weak. The dynamics that develops at those time scales thus mostly reflects intrinsic ocean processes. We estimate the amplitude of this intrinsic variability by examining one member of the ensemble OCAC. This

---

<sup>2</sup>Note that here, the forced origin of this South Atlantic dynamics on the North Atlantic subtropical AMOC variability results from our regional model strategy. It does not question the intrinsic origin of this variability in the real ocean, as proposed by others with global simulations (Bjastoch et al. 2008b; Hirschi et al. 2013; Grégorio et al. 2015; Leroux et al. 2018).

ensemble is driven by yearly repeating atmospheric forcing and open boundary conditions, providing an estimate of the signals that develop in our regional configuration at low-frequency that cannot be interpreted as forced. Within this ensemble, member #02 exhibits the strongest intrinsic variability within the subtropical gyre. We thus use this member to maximize our estimates of AMOC variability that cannot be interpreted as forced. Additionally, we previously identified that the boundary forced AMOC signals dominate at decadal time scales; therefore, we now focus our discussion in this frequency band.

AMOC anomalies at 1200 m depth are shown in Fig. 9 as latitude-time Hovmöller diagrams. Comparing AMOC anomalies in the two single simulations runN and runS with the ORAC ensemble mean strongly suggests that our decadal boundary forced AMOC variability is mostly driven by signals entering the domain through the northern boundary. The simulation runN exhibits indeed a marked strengthening during the late nineties very comparable to the AMOC variability diagnosed in the ORAC ensemble mean, although less regular in time due to the presence of interannual intrinsic variability. In contrast, no such signal is found in runS, suggesting a weaker impact of southern origin dynamics for the overall North Atlantic subtropical AMOC variability. Also note that our detrending procedure has removed very low-frequency AMOC signals (not shown). At 26.5°N, this very low-frequency variability exhibits a strengthening of the AMOC maximum up to the mid- 1990's of about 1 Sv, and a decay afterward. This signal is observed in both the ORAC ensemble mean and in runN, consistent with what can be found in ocean models of the CORE-II experiments (Danabasoglu et al. 2016). In contrast, we did not find evidence of such a signal in runS, suggesting here again the leading role of subpolar North Atlantic dynamics for the low-frequency AMOC variability within the North Atlantic subtropical gyre.

Finally, although the imprint of the southern boundary on the forced AMOC variability is globally weak, its contribution, not surprisingly, prevails in the southern part of our regional domain.

South of the equator, intrinsic AMOC variability is weak ( $\sigma = 0.3$  Sv; Fig. 9 top right panel), such that AMOC anomalies observed in runS can be interpreted as driven by our southern boundary. At these latitudes, AMOC variability in runN is also weaker ( $\sigma = 0.5$  and  $\sigma = 0.8$  Sv for runN and runS, respectively), and does not explain the 0.7 Sv AMOC standard deviation diagnosed in the ORAC ensemble mean. In contrast with the northern boundary, the signal imprinted by the southern boundary contains energy at interannual time scales. This is visible in the Hovmöller diagrams of both the ensemble mean  $\langle \text{ORAC} \rangle$  and of runS, as well as in the spectral estimates of AMOC variability (Fig. 6, bottom left panel). In the North Atlantic subtropical gyre, the AMOC variance is slightly larger in the runS than in OCAC ensemble member #02 ( $\sigma = 1$  Sv and  $\sigma = 0.8$  Sv, respectively), suggesting a weak contribution of about 0.1-0.2 Sv for the overall subtropical AMOC variability. This would suggest that, although their imprint are weak, South Atlantic signals could make their way through the equator and contribute to AMOC variability further north. Those results are consistent with earlier studies (Biaosoch et al. 2008b; Leroux et al. 2018), but we are not able to robustly investigate such a northward propagation route with a single, eddy resolving simulation. Further investigations are thus required to support those preliminary estimates of the contribution of South Atlantic dynamics for the North Atlantic subtropical AMOC variability.

## 7. Summary and discussion

We analyzed in this study the results of four ensemble simulations of a regional ( $20^{\circ}\text{S}$ - $55^{\circ}\text{N}$ ) configuration of the North Atlantic. This analysis focused on the origin (local or remote) of the forced, low-frequency (2-30 years) variability of the Atlantic Meridional Overturning Circulation (AMOC) in the subtropical gyre. Simulations have been carried out at eddy-resolving resolution ( $\frac{1}{12}^{\circ}$ ) to account for the role of eddies in the general ocean circulation. Ensemble statistics have thus been applied to isolate the AMOC signals driven by forcing from those with an intrinsic

548 origin due to non-linear dynamics explicitly resolved at this resolution. The four ensembles have  
549 been exposed to different forcing, where we have alternatively permuted surface and boundary  
550 forcing from fully varying (realistic) to yearly repeating signals. Comparing the AMOC variability  
551 simulated by these four ensembles allow us to disentangle the respective contribution of low-  
552 frequency atmospheric forcing from signals with a remote origin and entering the domain through  
553 the boundaries. The main results can be summarized as follow:

- 554 1. Isolating the variability driven by the local atmospheric forcing from the variability driven by  
555 open boundaries revealed a pronounced time scale separation: The leading mode of AMOC  
556 variability driven by local surface forcing dominates at interannual (2-10 years) time scales,  
557 while that driven by open boundaries dominates at decadal (10-30 years) time scales. Due to  
558 the stronger imprint of the local atmospheric forcing, the leading mode of AMOC variability  
559 in realistic conditions (i.e. with both realistic surface and realistic boundary forcing) extracted  
560 through PCA mostly reflects the imprint of the atmosphere.
- 561 2. The marked time scale separation between surface and boundary forcing allows for a good  
562 reproduction of the realistic AMOC variability in most of the subtropical gyre through a  
563 linear combination of surface and boundary forced signals. Peculiarities emerged however at  
564 the subtropical-subpolar intergyre position. There, the imprint of the atmosphere is found to  
565 extend at decadal time scales, and interact with the boundary forced signal.
- 566 3. Although marked differences appeared in the forced (ensemble mean) AMOC variability,  
567 all ensembles exhibit a very similar intrinsic (ensemble spread) AMOC variability. They  
568 all reproduce a basin scale mode of intrinsic AMOC variability peaking at 20°N and 2000  
569 m depth, with an interannual time scales. This highlights the very weak sensitivity of this

intrinsic mode to the surrounding forced AMOC variability, and thus no causal relationship between the two.

4. Both northern and southern boundaries are found to contribute to AMOC variability within our domain, although with different amplitude. Overall, the contribution of northern origin signals dominates, particularly at the RAPID site ( $26.5^{\circ}\text{N}$ ), but southern origin signals might well contribute at second order.

These results bring new insights in the partitioning of the subtropical AMOC variability. Although the sensitivity experiments on the southern or northern origin of the boundary forced AMOC variability suggest a stronger imprint of the northern boundary signal for AMOC variability at  $26.5^{\circ}\text{N}$ , they also support the earlier findings of Biastoch et al. (2008b) and Leroux et al. (2018) where the southern boundary is found to imprint a weak AMOC variability at  $26.5^{\circ}\text{N}$ , with a likely intrinsic origin (Leroux et al. 2018). Such a contribution is suggested to be of the order of 0.1-0.2 Sv, consistent with their earlier estimates. Dedicated studies are however required to provide a robust estimate of the imprint of the South Atlantic dynamics on the subtropical AMOC variability, thus helping the interpretation of the RAPID-MOCHA-WBTS time series. For this purpose, a filtering procedure could be developed to consistently filter intrinsic AMOC variability, such as what Close et al. (2020) proposed to separate forced and intrinsic variability of the sea surface height. Applying such a filtering procedure to the AMOC time series would first reduce the computational time required to extract forced AMOC signals from single, eddy resolving simulations, and would also help interpreting the forced component of AMOC variability as observed by the RAPID-MOCHA-WBTS (McCarthy et al. 2015b) or the OSNAP (Lozier et al. 2017) arrays.

Finally, we would like to further discuss the implications of our results at the intergyre position. We found that the atmosphere drives AMOC variability at decadal time scales in the  $30\text{-}40^{\circ}$  lat-

itude band, which interacts with the decadal scale signals driven by boundaries. As a result, the realistic AMOC variability in this region cannot be reconstructed through a linear combination of these two signals. These results are in line with the complex dynamics associated with the crossover of the Gulf Stream and the Deep Western Boundary Current (Spall 1996a,b; Bower and Hunt 2000; Zhang and Vallis 2007; Andres et al. 2016). From a Lagrangian point of view however, modifications of DWBC signals through interaction with the Gulf Stream are expected to imprint further south as those signals propagate along the western boundary. However, within the subtropical gyre, we found that the linear reconstruction leads to consistent estimates of the realistic low-frequency AMOC variability. These results thus question on the role played by the complex dynamics at the intergyre position for the low-frequency AMOC variability of the subtropical gyre, thus for the interpretation of the RAPID array time series.

*Acknowledgments.* This work has been founded by the NSF award OCE-1537304, and by the 'Make Our Planet Great Again' CONTaCTS project led by William K. Dewar. Highperformance computing resources on Cheyenne (doi:10.5065/D6RX99HX) have been provided by NCAR's Computational and Information Systems Laboratory, sponsored by the National Science Foundation, under the university large allocations UFSU0011. We also thank Bernard Barnier from l'Institut des Géosciences de l'Environnement (IGE, Grenoble, France) and his collaborators for providing necessary data to force our regional model, and Stephanie Leroux from Ocean Next for fruitful discussions during the preparation of this manuscript. Data from the RAPID AMOC monitoring project are funded by the Natural Environment Research Council and are freely available from [www.rapid.ac.uk/rapidmoc](http://www.rapid.ac.uk/rapidmoc). The simulations used in this study are available at [http://ocean.fsu.edu/~qjamet/share/data/forced\\_amoc\\_2019/](http://ocean.fsu.edu/~qjamet/share/data/forced_amoc_2019/).

## References

- Andres, M., J. Toole, D. Torres, W. Smethie Jr, T. Joyce, and R. Curry, 2016: Stirring by deep cyclones and the evolution of Denmark Strait Overflow Water observed at Line W. *Deep Sea Research Part I: Oceanographic Research Papers*, **109**, 10–26.
- Balmaseda, M. A., G. C. Smith, K. Haines, D. Anderson, T. N. Palmer, and A. Vidard, 2007: Historical reconstruction of the Atlantic Meridional Overturning Circulation from the ECMWF operational ocean reanalysis. *Geophys. Res. Lett.*, **34** (23).
- Barrier, N., A.-M. Treguier, C. Cassou, and J. Deshayes, 2013: Impact of the winter North-Atlantic weather regimes on subtropical sea-surface height variability. *Clim. Dyn.*, **41** (5-6), 1159–1171.
- Biastoch, A., C. W. Böning, J. Getzlaff, J.-M. Molines, and G. Madec, 2008a: Causes of interannual–decadal variability in the meridional overturning circulation of the midlatitude North Atlantic Ocean. *J. Clim.*, **21** (24), 6599–6615.
- Biastoch, A., C. W. Böning, and J. Lutjeharms, 2008b: Agulhas leakage dynamics affects decadal variability in Atlantic overturning circulation. *Nature*, **456** (7221), 489.
- Bower, A. S., and H. D. Hunt, 2000: Lagrangian observations of the deep western boundary current in the North Atlantic Ocean. Part II: The Gulf Stream–deep western boundary current crossover. *J. Phys. Oceanogr.*, **30** (5), 784–804.
- Bower, A. S., M. S. Lozier, S. F. Gary, and C. W. Böning, 2009: Interior pathways of the North Atlantic meridional overturning circulation. *Nature*, **459** (7244), 243.
- Brodeau, L., B. Barnier, A.-M. Treguier, T. Penduff, and S. Gulev, 2010: An ERA40-based atmospheric forcing for global ocean circulation models. *Ocean Modelling*, **31** (3-4), 88–104.

636 Buckley, M. W., D. Ferreira, J.-M. Campin, J. Marshall, and R. Tulloch, 2012: On the relationship  
637 between decadal buoyancy anomalies and variability of the Atlantic meridional overturning  
638 circulation. *J. Clim.*, **25** (23), 8009–8030.

639 Cabanes, C., T. Lee, and L.-L. Fu, 2008: Mechanisms of interannual variations of the meridional  
640 overturning circulation of the North Atlantic Ocean. *J. Phys. Oceanogr.*, **38** (2), 467–480.

641 Close, S., T. Penduff, S. Speich, and J.-M. Molines, 2020: A means of estimating the intrinsic  
642 and atmospherically-forced contributions to sea surface height variability applied to altimetric  
643 observations. *Prog. Oceanogr.*, – (–), –.

644 Czaja, A., and J. Marshall, 2001: Observations of atmosphere-ocean coupling in the North At-  
645 lantic. *Quarterly Journal of the Royal Meteorological Society*, **127** (576), 1893–1916.

646 Danabasoglu, G., and Coauthors, 2014: North Atlantic simulations in coordinated ocean-ice ref-  
647 erence experiments phase II (CORE-II). Part I: mean states. *Ocean Modelling*, **73**, 76–107.

648 Danabasoglu, G., and Coauthors, 2016: North Atlantic simulations in Coordinated Ocean-ice  
649 Reference Experiments phase II (CORE-II). Part II: Inter-annual to decadal variability. *Ocean*  
650 *Modelling*, **97**, 65–90.

651 Deremble, B., N. Wienders, and W. Dewar, 2013: CheapAML: A simple, atmospheric boundary  
652 layer model for use in ocean-only model calculations. *Mon. Wea. Rev.*, **141** (2), 809–821.

653 Deshayes, J., and C. Frankignoul, 2005: Spectral characteristics of the response of the meridional  
654 overturning circulation to deep-water formation. *J. Phys. Oceanogr.*, **35** (10), 1813–1825.

655 Deshayes, J., and C. Frankignoul, 2008: Simulated variability of the circulation in the North  
656 Atlantic from 1953 to 2003. *J. Clim.*, **21** (19), 4919–4933.

657 Dussin, R., B. Barnier, L. Brodeau, and J. Molines, 2016: The making of the Drakkar Forcing Set  
658 DFS5. *DRAKKAR/MyOcean Rep. 01–04*, **16**.

659 Eden, C., and T. Jung, 2001: North Atlantic interdecadal variability: Oceanic response to the  
660 North Atlantic Oscillation (1865-1997). *J. Clim.*, **14**, 676–691.

661 Eden, C., and J. Willebrand, 2001: Mechanism of interannual to decadal variability of the North  
662 Atlantic circulation. *J. Clim.*, **14** (10), 2266–2280.

663 Fairall, C., E. F. Bradley, J. Hare, A. Grachev, and J. Edson, 2003: Bulk parameterization of  
664 air–sea fluxes: Updates and verification for the COARE algorithm. *J. Clim.*, **16** (4), 571–591.

665 Frajka-Williams, E., S. Cunningham, H. Bryden, and B. King, 2011: Variability of Antarctic  
666 bottom water at 24.5 N in the Atlantic. *Journal of Geophysical Research: Oceans*, **116** (C11).

667 Gastineau, G., and C. Frankignoul, 2012: Cold-season atmospheric response to the natural vari-  
668 ability of the Atlantic Meridional Overturning Circulation. *Clim. Dyn.*, **39** (1-2), 37–57.

669 Goldenberg, S. B., C. W. Landsea, A. M. Mestas-Núñez, and W. M. Gray, 2001: The recent  
670 increase in Atlantic hurricane activity: Causes and implications. *Science*, **293** (5529), 474–479.

671 Grégorio, S., T. Penduff, G. Sérazin, J.-M. Molines, B. Barnier, and J. Hirschi, 2015: Intrinsic  
672 Variability of the Atlantic Meridional Overturning Circulation at Interannual-to-Multidecadal  
673 Time Scales. *Journal of Physical Oceanography*, **45** (7), 1929–1946.

674 Häkkinen, S., 2001: Variability in sea surface height: A qualitative measure for the meridional  
675 overturning in the North Atlantic. *Journal of Geophysical Research: Oceans*, **106** (C7), 13 837–  
676 13 848.

677 Hallam, S., R. Marsh, S. A. Josey, P. Hyder, B. Moat, and J. J.-M. Hirschi, 2019: Ocean precursors  
678 to the extreme atlantic 2017 hurricane season. *Nature communications*, **10** (1), 1–10.

679 Hirschi, J., and J. Marotzke, 2007: Reconstructing the meridional overturning circulation from  
680 boundary densities and the zonal wind stress. *J. Phys. Oceanogr.*, **37** (3), 743–763.

681 Hirschi, J. J.-M., A. T. Blaker, B. Sinha, A. C. Coward, B. A. De Cuevas, S. G. Alderson, and  
682 G. Madec, 2013: Chaotic variability of the meridional overturning circulation on subannual to  
683 interannual timescales. **9** (2), 805–823.

684 Hodson, D. L., and R. T. Sutton, 2012: The impact of resolution on the adjustment and decadal  
685 variability of the Atlantic meridional overturning circulation in a coupled climate model. *Clim.*  
686 *Dyn.*, **39** (12), 3057–3073.

687 Jamet, Q., W. Dewar, N. Wienders, and B. Deremble, 2019: Fast warming of the surface ocean  
688 under a climatological scenario. *Geophys. Res. Lett.*, **46** (7), 3871–3879.

689 Jamet, Q., W. Dewar, N. Wienders, and B. Deremble, 2019b: Spatio-temporal patterns of Chaos  
690 in the Atlantic Overturning Circulation. *Geophys. Res. Lett.*, **46** (13), 7509–7517.

691 Jamet, Q., T. Huck, O. Arzel, J.-M. Campin, and A. Colin de Verdière, 2016: Oceanic control of  
692 multidecadal variability in an idealized coupled GCM. *Clim. Dyn.*, **46** (9), 3079–3095.

693 Johnson, H. L., and D. P. Marshall, 2002: A theory for the surface Atlantic response to thermoha-  
694 line variability. *J. Phys. Oceanogr.*, **32** (4), 1121–1132.

695 Kawase, M., 1987: Establishment of deep ocean circulation driven by deep-water production. *J.*  
696 *Phys. Oceanogr.*, **17** (12), 2294–2317.

697 Kerr, R. A., 2000: A North Atlantic climate pacemaker for the centuries. *Science*, **288** (5473),  
698 1984–1985.

699 Knight, J. R., R. J. Allan, C. K. Folland, M. Vellinga, and M. E. Mann, 2005: A signature  
700 of persistent natural thermohaline circulation cycles in observed climate. *Geophys. Res. Lett.*,  
701 **32 (L20708)**.

702 Kostov, Y., and Coauthors, Sub.: Contrasting sources of variability in subtropical and subpolar  
703 Atlantic overturning. *Nature Geoscience*, – (–), –.

704 Kushnir, Y., 1994: Interdecadal variations in North Atlantic sea surface temperature and associated  
705 atmospheric conditions. *J. Clim.*, **7 (1)**, 141–157.

706 Large, W. G., and S. G. Yeager, 2004: Diurnal to decadal global forcing for ocean and sea-ice  
707 models: the data sets and flux climatologies.

708 Leroux, S., T. Penduff, L. Bessi eres, J.-M. Molines, J.-M. Brankart, G. S erazin, B. Barnier, and  
709 L. Terray, 2018: Intrinsic and Atmospherically Forced Variability of the AMOC: Insights from  
710 a Large-Ensemble Ocean Hindcast. *Journal of Climate*, **31 (3)**, 1183–1203.

711 Lozier, M., and Coauthors, 2019: A sea change in our view of overturning in the subpolar North  
712 Atlantic. *Science*, **363 (6426)**, 516–521.

713 Lozier, M. S., 2010: Deconstructing the conveyor belt. *Science*, **328 (5985)**, 1507–1511.

714 Lozier, S. M., and Coauthors, 2017: Overturning in the Subpolar North Atlantic Program: A new  
715 international ocean observing system. *Bull. Am. Met. Soc.*, **98 (4)**, 737–752.

716 Marshall, J., A. Adcroft, C. Hill, L. Perelman, and C. Heisey, 1997: A finite-volume, incom-  
717 pressible Navier Stokes model for studies of the ocean on parallel computers. *J. Geophys. Res.*,  
718 **102 (C3)**, 5753–5766.

719 McCarthy, G., and Coauthors, 2015a: Measuring the Atlantic meridional overturning circulation  
720 at 26 N. *Prog. Oceanogr.*, **130**, 91–111.

721 McCarthy, G. D., I. D. Haigh, J. J.-M. Hirschi, J. P. Grist, and D. A. Smeed, 2015b: Ocean impact  
 722 on decadal Atlantic climate variability revealed by sea-level observations. *Nature*, **521 (7553)**,  
 723 508–510.

724 Menary, M. B., L. Hermanson, and N. J. Dunstone, 2016: The impact of labrador sea tempera-  
 725 ture and salinity variability on density and the subpolar amoc in a decadal prediction system.  
 726 *Geophys. Res. Lett.*, **43 (23)**, 12–217.

727 Molines, J., B. Barnier, T. Penduff, A. Treguier, and J. Le Sommer, 2014: ORCA12. L46 cli-  
 728 matological and interannual simulations forced with DFS4. 4: GJM02 and MJM88. Drakkar  
 729 Group Experiment Rep. Tech. rep., GDRI-DRAKKAR-2014-03-19, 50 pp.[Available online at  
 730 [http://www.drakkar-ocean.eu/publications/reports/orca12\\_reference\\_experiments\\_2014.](http://www.drakkar-ocean.eu/publications/reports/orca12_reference_experiments_2014.)].

731 Muir, L. C., and A. V. Fedorov, 2016: Evidence of the AMOC interdecadal mode related to west-  
 732 ward propagation of temperature anomalies in CMIP5 models. *Clim. Dyn.*, **in press**, 1–19,  
 733 doi:10.1007/s00382-016-3157-9.

734 Reintges, A., M. Latif, and W. Park, 2017: Sub-decadal North Atlantic Oscillation variability in  
 735 observations and the Kiel climate model. *Clim. Dyn.*, **48 (11-12)**, 3475–3487.

736 Roberts, C., and Coauthors, 2013: Atmosphere drives recent interannual variability of the Atlantic  
 737 meridional overturning circulation at 26.5 N. *Geophysical Research Letters*, **40 (19)**, 5164–  
 738 5170.

739 Schlesinger, M. E., and N. Ramankutty, 1994: An oscillation in the global climate system of period  
 740 65-70 years. *Nature*, **367 (6465)**, 723–726.

741 Schott, F. A., R. Zantopp, L. Stramma, M. Dengler, J. Fischer, and M. Wibaux, 2004: Circulation  
 742 and deep-water export at the western exit of the subpolar North Atlantic. *J. Phys. Oceanogr.*,  
 743 **34 (4)**, 817–843.

744 Send, U., M. Lankhorst, and T. Kanzow, 2011: Observation of decadal change in the Atlantic  
 745 meridional overturning circulation using 10 years of continuous transport data. *Geophys. Res.*  
 746 *Lett.*, **38 (24)**.

747 Smeed, D., and Coauthors, 2014: Observed decline of the Atlantic meridional overturning circu-  
 748 lation 2004–2012. *Ocean Science*, **10 (1)**, 29–38.

749 Smeed, D., and Coauthors, 2018: The North Atlantic Ocean is in a state of reduced overturning.  
 750 *Geophysical Research Letters*, **45 (3)**, 1527–1533.

751 Spall, M. A., 1996a: Dynamics of the Gulf Stream/deep western boundary current crossover. Part  
 752 I: Entrainment and recirculation. *J. Phys. Oceanogr.*, **26 (10)**, 2152–2168.

753 Spall, M. A., 1996b: Dynamics of the Gulf Stream/deep western boundary current crossover. Part  
 754 II: Low-frequency internal oscillations. *J. Phys. Oceanogr.*, **26 (10)**, 2169–2182.

755 Sutton, R. T., and B. Dong, 2012: Atlantic Ocean influence on a shift in European climate in the  
 756 1990s. *Nature Geoscience*, **5 (11)**, 788.

757 Tulloch, R., and J. Marshall, 2012: Exploring mechanisms of variability and predictability of  
 758 Atlantic meridional overturning circulation in two coupled climate models. *J. Clim.*, **25 (12)**,  
 759 4067–4080.

760 Wunsch, C., 2013: Covariances and linear predictability of the Atlantic Ocean. *Deep Sea Research*  
 761 *Part II: Topical Studies in Oceanography*, **85**, 228–243.

Wunsch, C., and P. Heimbach, 2013: Two decades of the Atlantic meridional overturning circulation: Anatomy, variations, extremes, prediction, and overcoming its limitations. *J. Clim.*, **26** (18), 7167–7186.

Zhang, R., 2008: Coherent surface-subsurface fingerprint of the Atlantic meridional overturning circulation. *Geophys. Res. Lett.*, **35** (L20705).

Zhang, R., 2010: Latitudinal dependence of Atlantic meridional overturning circulation (AMOC) variations. *Geophys. Res. Lett.*, **37** (L16703).

Zhang, R., 2017: On the persistence and coherence of subpolar sea surface temperature and salinity anomalies associated with the atlantic multidecadal variability. *Geophys. Res. Lett.*, **44** (15), 7865–7875.

Zhang, R., and T. L. Delworth, 2006: Impact of Atlantic multidecadal oscillations on India/Sahel rainfall and Atlantic hurricanes. *Geophysical Research Letters*, **33** (17).

Zhang, R., and G. K. Vallis, 2007: The role of bottom vortex stretching on the path of the North Atlantic western boundary current and on the northern recirculation gyre. *J. Phys. Oceanogr.*, **37** (8), 2053–2080.

Zhao, J., and W. Johns, 2014: Wind-forced interannual variability of the Atlantic Meridional Overturning Circulation at 26.5° N. *Journal of Geophysical Research: Oceans*, **119** (4), 2403–2419.

Zou, S., and M. S. Lozier, 2016: Breaking the linkage between Labrador Sea Water production and its advective export to the subtropical gyre. *J. Phys. Oceanogr.*, **46** (7), 2169–2182.

782	<b>LIST OF TABLES</b>	
783	<b>Table 1.</b> Summary of the simulations discussed in this study, where $\langle . \rangle$ indicates	
784	ensemble simulations. . . . .	38

TABLE 1. Summary of the simulations discussed in this study, where < . > indicates ensemble simulations.

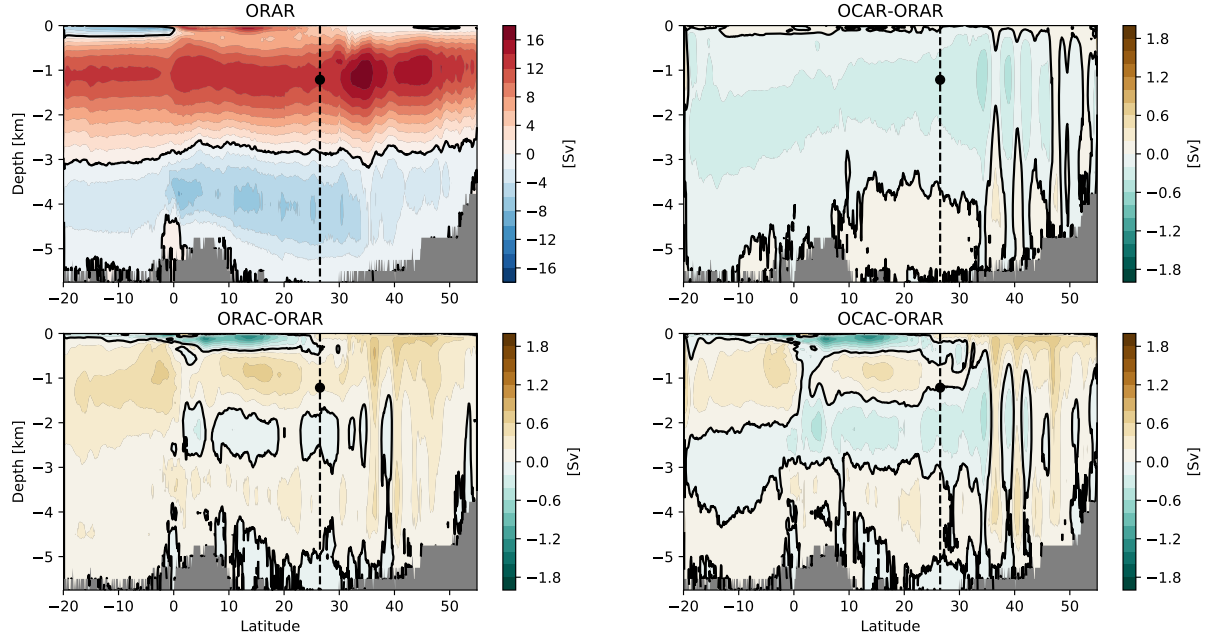
Atmosphere Open Boundary	Fully varying	Normal year
Fully varying	<ORAR>	<ORAC>
Climatologic	<OCAR>	<OCAC>
Northern boundary real		runN
Southern boundary real		runS

## LIST OF FIGURES

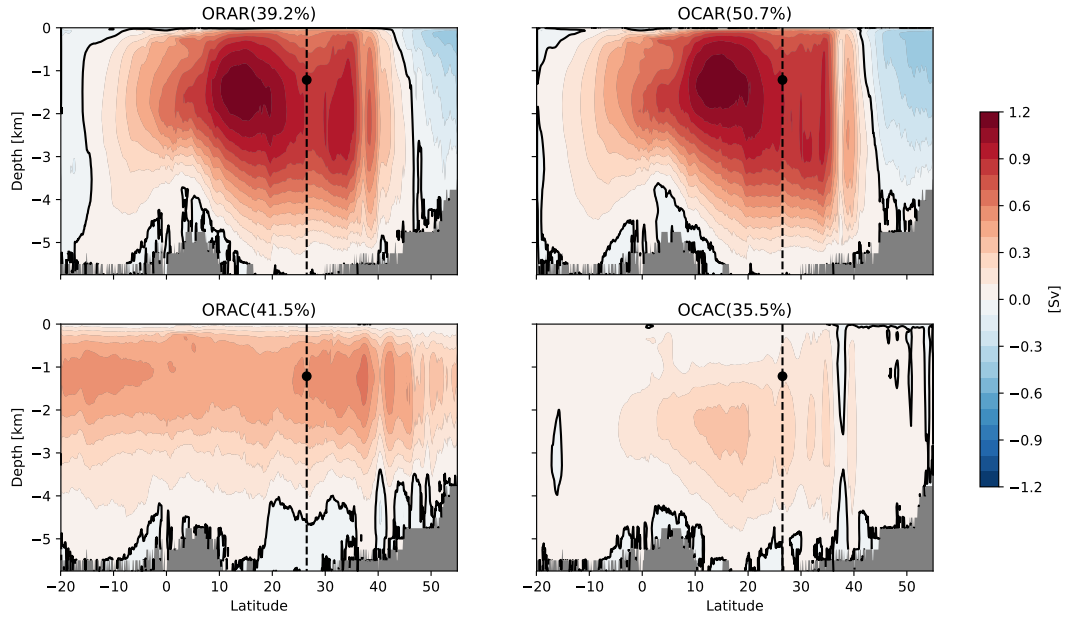
- Fig. 1.** Time mean Atlantic Meridional Overturning Circulation (AMOC) streamfunction for the reference, realistic ensemble ORAR (top left, contour interval = 2 Sv), and associated departures from this reference ensemble for the 3 other ensembles OCAR (top right), ORAC (bottom left) and OCAC (bottom right; contour interval = 0.2 Sv). See Table 1 for further details on the experiments. Zero contours are in black. The dashed line represents the location of the RAPID-MOCHA-WBTS array, and the black dot the depth of the maximum time mean AMOC used in Fig. 6. The time mean AMOC is computed from the ensemble mean, unprocessed, 5-day averaged model outputs. . . . . 41
- Fig. 2.** Leading modes of the ensemble mean AMOC variability in the four ensembles ORAR (top left), OCAR (top right), ORAC (bottom left) and OCAC (bottom right). Empirical Orthogonal Functions (EOFs) have been normalized by the standard deviation of their associated Principal Components (PCs) such that they contain the amplitude, in Sv, of the explained signal. Zero contours are in black and contour interval is 0.1 Sv. The dashed line represents the location of the RAPID-MOCHA-WBTS array, and the black dot the depth of the maximum time mean AMOC. . . . . 42
- Fig. 3.** Temporal standard deviation of the ensemble mean AMOC for the ensemble ORAR (top left), OCAR (top right), ORAC (bottom left) and OCAC (bottom right). Contour interval is 0.1 Sv. The dashed line represents the location of the RAPID-MOCHA-WBTS. The temporal standard deviation is computed from the ensemble mean, time processed (band-passed filtered and deseasonalized) AMOC. . . . . 43
- Fig. 4.** Time series of the PCs associated with the leading mode of variability presented on Fig. 2 (left), and their associated Power Spectral Density (PSD) function (right). Normalized PCs have been multiplied by the respective maximum of their associated EOFs to account for their magnitude. . . . . 44
- Fig. 5.** (Top) Times series of the ensemble mean AMOC anomalies at 26.5°N and 1200 m depth in the four ensembles (left), and their associated PSD functions (right). PSD functions have been smoothed with a 5-point moving average window. 1-year low-pass filtered RAPID array time series is shown in purple for comparison. (Bottom) Same as top but for the realistic ensemble ORAR (black), with  $\pm$  one standard deviation associated with the ensemble spread (grey shading), and a reconstruction made as the sum of the two ensembles mean ORAC+OCAR (cyan). . . . . 45
- Fig. 6.** Ensemble mean AMOC PSD functions as a function of latitude at 1200 m depth for the three ensembles ORAR (top left), OCAR (top right), and ORAC (bottom left). Grey contours on top left panel show the PSD of the reconstructed AMOC as a combination of the two ensembles ORAC+OCAR, and the error in the reconstructed spectral content is shown on the bottom right panel. Blue colors indicate that the PSD of the reconstructed AMOC time series exceeds that of the realistic ensemble. PSD functions have been smoothed with a 5-point moving average window. The black line indicates the latitude of 26.5°N. . . . . 46
- Fig. 7.** Correlation coefficients between the realistic experiment ORAR and the linear reconstruction OCAR+ORAC for (left) the ensemble mean and (middle) memb#00 only. (right) Correlations at the depth of 1200 m for the ensemble mean (red) and memb#00 only (grey). 47
- Fig. 8.** (Top) Leading mode of intrinsic AMOC variability for the 4 ensembles ORAR (top left), OCAR (top right), ORAC (bottom left) and OCAC (bottom right). EOFs have been normal-

ized by the standard deviation of their associated PCs such that they contain the amplitude, in Sv, of the explained signal. Zero contours are in black, contour interval is 0.1 Sv and the dashed line represents the location of the RAPID-MOCHA-WBTS array. (Bottom) Associated spectral content, computed as the ensemble-averaged PSD functions of the normalized PCs multiplied by the maximum of their associated EOF. . . . . 48

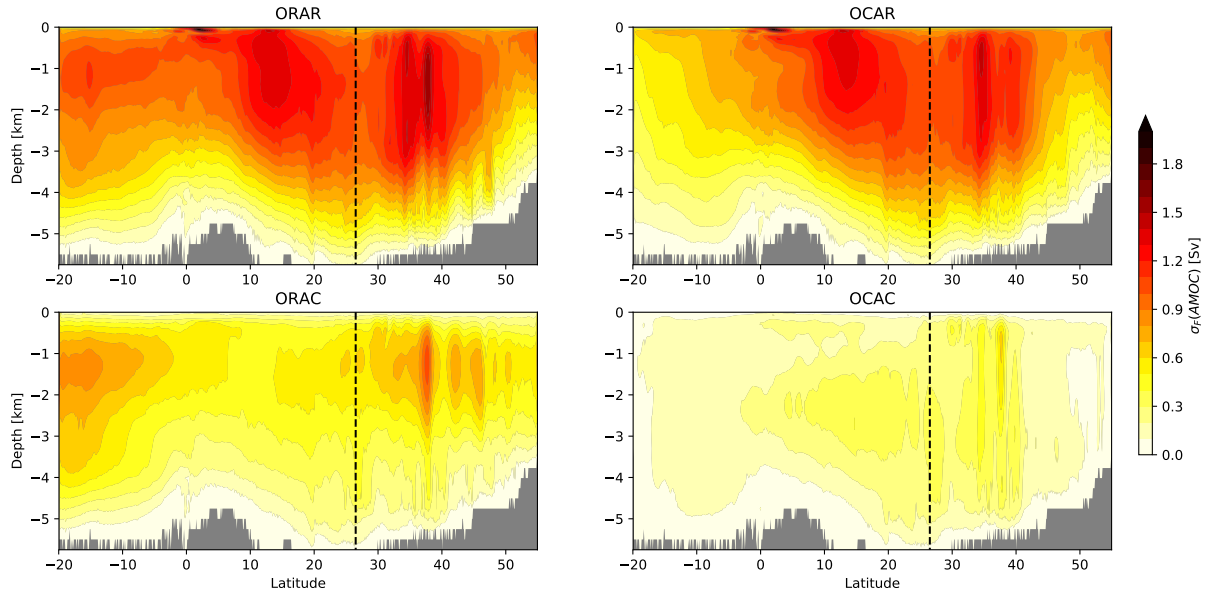
**Fig. 9.** Latitude-time Hovmöller diagrams of AMOC anomalies at 1200 m depth for (top left) the ORAC ensemble mean, the  $\langle . \rangle$  indicates ensemble averaging, (top right) ensemble member #02 of the ensemble OCAC, and (bottom) the two additional, single simulations runN and runS. Contour interval is 0.5 Sv. Black dashed line indicates the latitude of 26.5°N. . . . 49



839 FIG. 1. Time mean Atlantic Meridional Overturning Circulation (AMOC) streamfunction for the reference,  
 840 realistic ensemble ORAR (top left, contour interval = 2 Sv), and associated departures from this reference  
 841 ensemble for the 3 other ensembles OCAR (top right), ORAC (bottom left) and OCAC (bottom right; contour  
 842 interval = 0.2 Sv). See Table 1 for further details on the experiments. Zero contours are in black. The dashed  
 843 line represents the location of the RAPID-MOCHA-WBTS array, and the black dot the depth of the maximum  
 844 time mean AMOC used in Fig. 6. The time mean AMOC is computed from the ensemble mean, unprocessed,  
 845 5-day averaged model outputs.



846 FIG. 2. Leading modes of the ensemble mean AMOC variability in the four ensembles ORAR (top left),  
 847 OCAR (top right), ORAC (bottom left) and OCAC (bottom right). Empirical Orthogonal Functions (EOFs)  
 848 have been normalized by the standard deviation of their associated Principal Components (PCs) such that they  
 849 contain the amplitude, in Sv, of the explained signal. Zero contours are in black and contour interval is 0.1 Sv.  
 850 The dashed line represents the location of the RAPID-MOCHA-WBTS array, and the black dot the depth of the  
 851 maximum time mean AMOC.



852 FIG. 3. Temporal standard deviation of the ensemble mean AMOC for the ensemble ORAR (top left), OCAR  
 853 (top right), ORAC (bottom left) and OCAC (bottom right). Contour interval is 0.1 Sv. The dashed line represents  
 854 the location of the RAPID-MOCHA-WBTS. The temporal standard deviation is computed from the ensemble  
 855 mean, time processed (band-passed filtered and deseasonalized) AMOC.

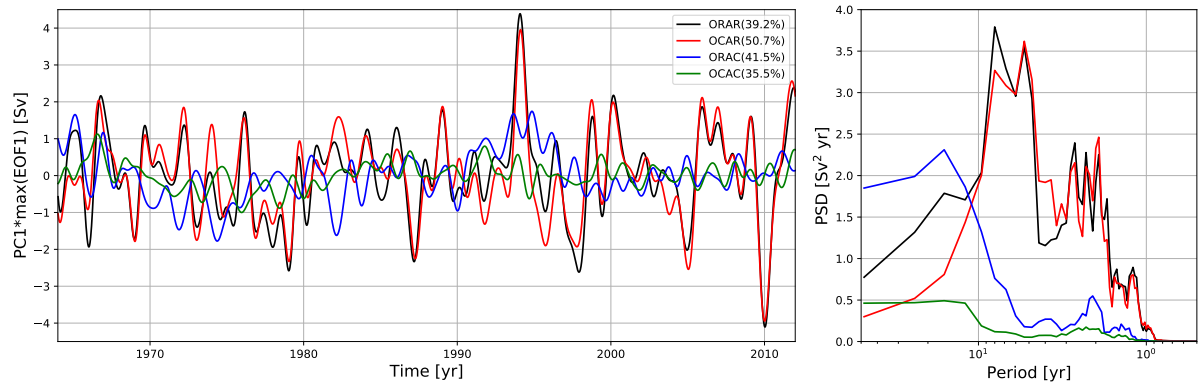
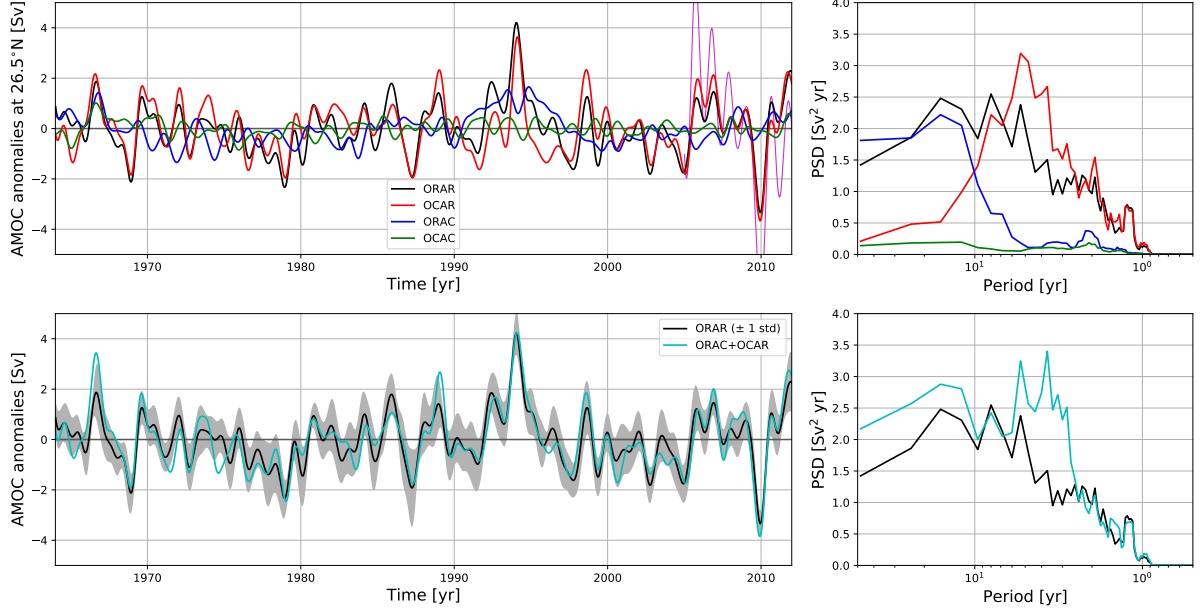
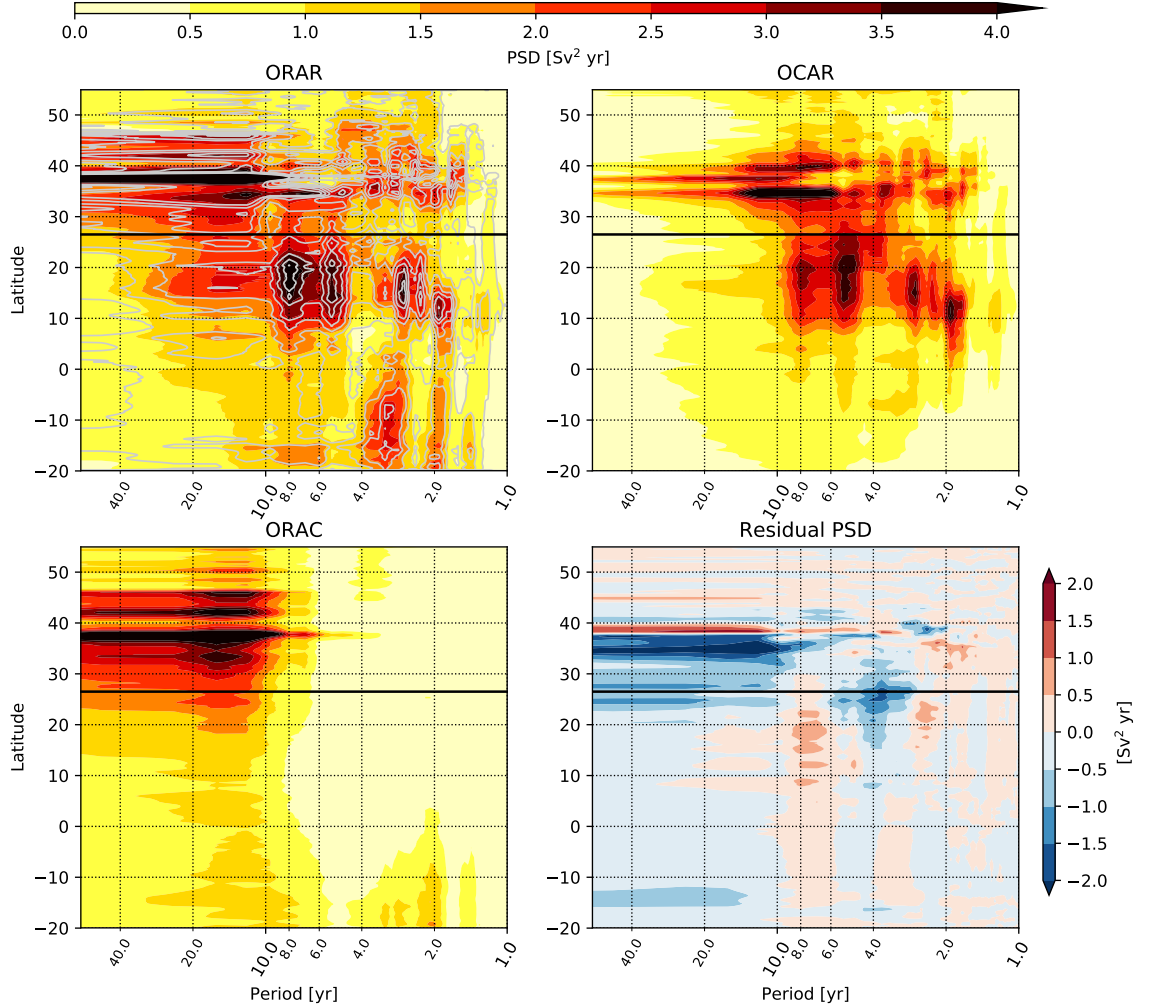


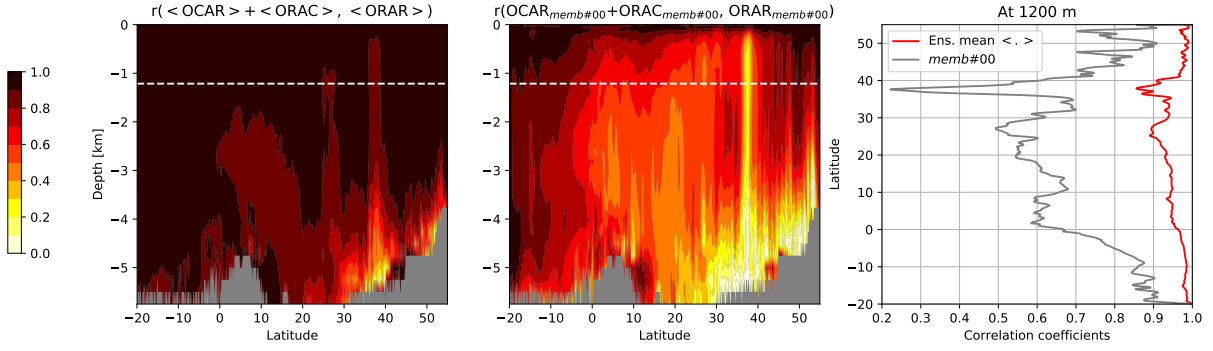
FIG. 4. Time series of the PCs associated with the leading mode of variability presented on Fig. 2 (left), and their associated Power Spectral Density (PSD) function (right). Normalized PCs have been multiplied by the respective maximum of their associated EOFs to account for their magnitude.



859 FIG. 5. (Top) Times series of the ensemble mean AMOC anomalies at  $26.5^{\circ}\text{N}$  and 1200 m depth in the four  
 860 ensembles (left), and their associated PSD functions (right). PSD functions have been smoothed with a 5-point  
 861 moving average window. 1-year low-pass filtered RAPID array time series is shown in purple for comparison.  
 862 (Bottom) Same as top but for the realistic ensemble ORAR (black), with  $\pm$  one standard deviation associated  
 863 with the ensemble spread (grey shading), and a reconstruction made as the sum of the two ensembles mean  
 864 ORAC+OCAR (cyan).



865 FIG. 6. Ensemble mean AMOC PSD functions as a function of latitude at 1200 m depth for the three en-  
 866 sembles ORAR (top left), OCAR (top right), and ORAC (bottom left). Grey contours on top left panel show  
 867 the PSD of the reconstructed AMOC as a combination of the two ensembles ORAC+OCAR, and the error in  
 868 the reconstructed spectral content is shown on the bottom right panel. Blue colors indicate that the PSD of the  
 869 reconstructed AMOC time series exceeds that of the realistic ensemble. PSD functions have been smoothed  
 870 with a 5-point moving average window. The black line indicates the latitude of 26.5°N.



871 FIG. 7. Correlation coefficients between the realistic experiment ORAR and the linear reconstruction  
 872 OCAR+ORAC for (left) the ensemble mean and (middle) memb#00 only. (right) Correlations at the depth  
 873 of 1200 m for the ensemble mean (red) and memb#00 only (grey).

# EOF1 intrinsic AMOC variability

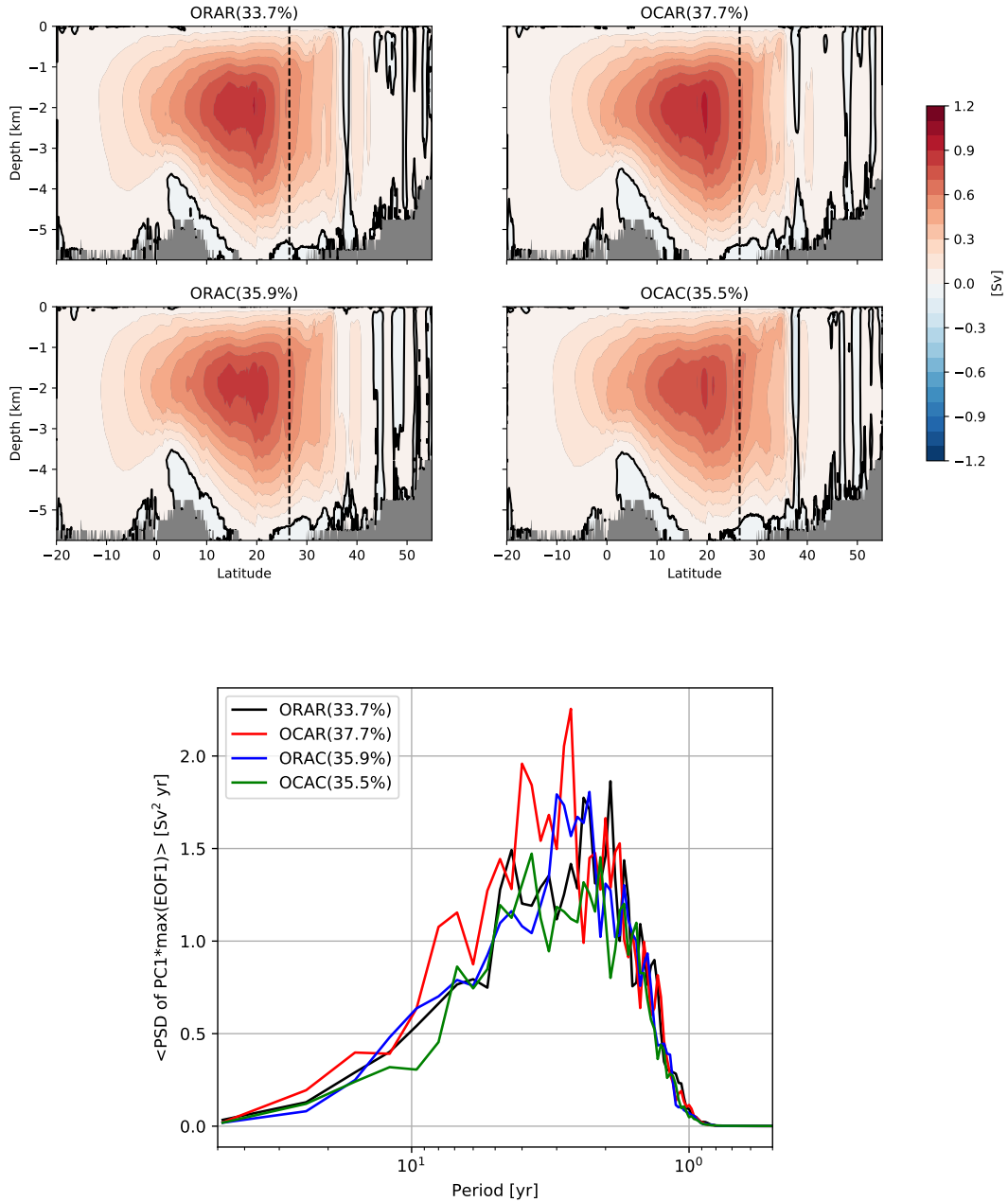
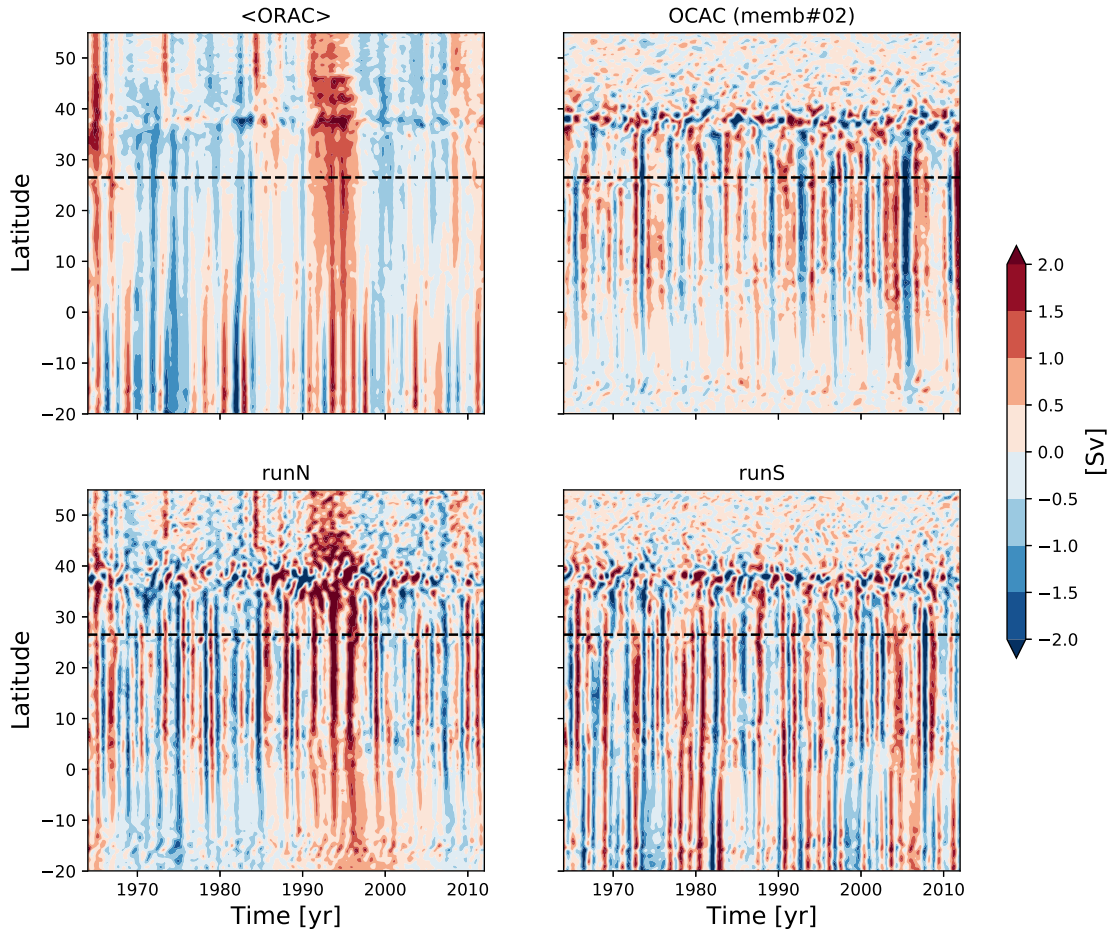


FIG. 8. (Top) Leading mode of intrinsic AMOC variability for the 4 ensembles ORAR (top left), OCAR (top right), ORAC (bottom left) and OCAC (bottom right). EOFs have been normalized by the standard deviation of their associated PCs such that they contain the amplitude, in Sv, of the explained signal. Zero contours are in black, contour interval is 0.1 Sv and the dashed line represents the location of the RAPID-MOCHA-WBTS array. (Bottom) Associated spectral content, computed as the ensemble-averaged PSD functions of the normalized PCs multiplied by the maximum of their associated EOF.



880 FIG. 9. Latitude-time Hovmöller diagrams of AMOC anomalies at 1200 m depth for (top left) the ORAC  
 881 ensemble mean, the  $\langle . \rangle$  indicates ensemble averaging, (top right) ensemble member #02 of the ensemble  
 882 OCAC, and (bottom) the two additional, single simulations runN and runS. Contour interval is 0.5 Sv. Black  
 883 dashed line indicates the latitude of  $26.5^\circ\text{N}$ .